Molecular Therapy
Methods & Clinical Development
Original Article

A T cell-targeted multi-antigen vaccine generates robust cellular and humoral immunity against SARS-CoV-2 infection

Stephen Boulton,[1,2] Joanna Poutou,[1,2] Rida Gill,[1] Nouf Alluqmani,[1,2] Xiaohong He,[1] Ragunath Singaravelu,[1,2] Mathieu J.F. Crupi,[1,2] Julia Petryk,[1] Bradley Austin,[1] Leonard Angka,[1] Zaid Taha,[1,2] Iris Teo,[1,3] Siddarth Singh,[1] Rameen Jamil,[1] Ricardo Marius,[1,2] Nikolas Martin,[1] Taylor Jamieson,[1,2] Taha Azad,[1,2,4,5] Jean-Simon Diallo,[1,2] Carolina S. Ilkow,[1,2] and John C. Bell[1,2]

[1]Ottawa Hospital Research Institute, Ottawa, ON K1H 8L6, Canada; [2]Department of Biochemistry, Microbiology and Immunology, University of Ottawa, Ottawa, ON K1H 8M5, Canada; [3]Department of Pathology and Laboratory Medicine, University of Ottawa, Ottawa, ON K1H 8M5, Canada; [4]Faculty of Medicine and Health Sciences, Department of Microbiology and Infectious Diseases, Université de Sherbrooke, Sherbrooke, QC J1E 4K8, Canada; [5]Centre de Recherche du CHUS, Sherbrooke, QC J1H 5N4, Canada

SARS-CoV-2, the etiological agent behind the coronavirus disease 2019 (COVID-19) pandemic, has continued to mutate and create new variants with increased resistance against the WHO-approved spike-based vaccines. With a significant portion of the worldwide population still unvaccinated and with waning immunity against newly emerging variants, there is a pressing need to develop novel vaccines that provide broader and longer-lasting protection. To generate broader protective immunity against COVID-19, we developed our second-generation vaccinia virus-based COVID-19 vaccine, TOH-VAC-2, encoded with modified versions of the spike (S) and nucleocapsid (N) proteins as well as a unique poly-epitope antigen that contains immunodominant T cell epitopes from seven different SARS-CoV-2 proteins. We show that the poly-epitope antigen restimulates T cells from the PBMCs of individuals formerly infected with SARS-CoV-2. In mice, TOH-VAC-2 vaccination produces high titers of S- and N-specific antibodies and generates robust T cell immunity against S, N, and poly-epitope antigens. The immunity generated from TOH-VAC-2 is also capable of protecting mice from heterologous challenge with recombinant VSV viruses that express the same SARS-CoV-2 antigens. Altogether, these findings demonstrate the effectiveness of our versatile vaccine platform as an alternative or complementary approach to current vaccines.

INTRODUCTION

The COVID-19 pandemic now enters its fourth year with a total number of cases exceeding 750 million and almost 7 million recorded deaths (https://covid19.who.int/). Despite the progress made in vaccine development and administration and the worldwide focus on public health safety, COVID-19 cases continue to soar. In December 2022, there were record-breaking levels of COVID-19 cases, higher than any other point during the pandemic. The record number of new cases has been brought on by the emergence of highly transmissible new variants, such as Omicron (B.1.1.529) and its sublineages, which quickly expanded through the world's population in 2022. In addition to its higher transmissibility, Omicron is less susceptible to pre-existing immunity from vaccination and prior infections with other SARS-CoV-2 strains. This is owed to the accumulation of more than 50 mutations, 36 of which are in the spike protein (S)—the primary antigen used in all WHO-approved COVID-19 vaccines.[1–5] Antibodies generated against the ancestral Wuhan S protein are less effective at recognizing and neutralizing Omicron S.[4–7] Even sublineages of Omicron have begun evolving to the point that neutralizing antibodies from older Omicron isolates (BA.1, BA.2) are less effective at neutralizing emerging variants.[4]

The continued development of COVID-19 vaccines is not only important to tackle emerging variants of concern (VOCs), but also for providing periodic boosters for immunocompromised individuals, whose protective immunity from vaccination is lower and diminishes much faster than normal individuals.[8,9] Adding to the challenge of vaccine resistance with new variants is the low rate of vaccination in lower-income countries. While multiple doses of monovalent and new bivalent vaccines offer some protection against Omicron variants, the number of people who have received even a single vaccine dose in low-income countries is less than 30%.[10] This is due to a combination of unequal vaccine access, supply chain

Received 2 May 2023; accepted 13 September 2023;
https://doi.org/10.1016/j.omtm.2023.101110.

Correspondence: Stephen Boulton, PhD, Ottawa Hospital Research Institute, Ottawa, ON K1H 8L6, Canada.
E-mail: sboulton@ohri.ca
Correspondence: Carolina S. Ilkow, PhD, Ottawa Hospital Research Institute, Ottawa, ON K1H 8L6, Canada.
E-mail: cilkow@ohri.ca
Correspondence: John C. Bell, PhD, Ottawa Hospital Research Institute, Ottawa, ON K1H 8L6, Canada.
E-mail: jbell@ohri.ca

problems, infrastructure challenges, and rising rates of vaccine hesitancy.[11,12] Vaccine hesitancy is also driven by the diminished efficacy of existing vaccines against emerging new variants, including significant drops in effective humoral responses 6 months post vaccination.[1,11] Periodic booster vaccinations are also recommended for immunocompromised individuals, such as those with diabetes, cancer, or AIDS. Hence, there is a pressing need to develop new vaccines that provide more durable immunity and maintain effectiveness against emergent SARS-CoV-2 variants. In addition, development of globally accessible vaccines that are easy to manufacture and distribute without the need for special infrastructure will help increase vaccination rates in low-income countries.

Previously, our group developed a COVID-19 vaccine using a vaccinia virus (VACV) vector encoded with S protein receptor binding domain (RBD) tethered to its C-terminal transmembrane region.[13] VACV was utilized as the vector because of its well-known safety profile from its extensive use during the worldwide smallpox vaccination campaign and its ability to effectively deliver heterologous antigens as immunogens.[14–16] Pre-existing immunity against the vector is also not a major concern, since it often does little to diminish immunity against heterologously expressed antigens.[17–20] Poxvirus vaccines are also easy to manufacture, stable over a range of temperatures, and can be freeze-dried for storage over extended periods without impacting their immunogenicity.[21–23] Both replicating (e.g., Tiantan, Lister, Wyeth, or Copenhagen) and non-replicating strains (e.g., MVA, NYVAC) of VACV have been utilized with great success as vaccine vectors, but non-replicating vectors such as modified vaccinia Ankara (MVA) are typically favored because of their improved safety.[24] However, we previously found that a replicating VACV vector (Tiantan; TT) vastly outperformed MVA in eliciting both humoral and T cell immunity against the RBD.[13] We showed that a single shot of the TT-based vaccine applied with a 10-fold lower dose elicited antibody production that was more than 1,000 times higher than those produced from MVA. Similarly, T cell responses against RBD epitopes were also significantly stronger when delivered via TT as opposed to MVA.[13] Through their extended growth and persistence, replication-competent vectors prolong antigen expression and increase T cell stimulation, which makes them ideal platforms for generating robust, long-lasting immunity.[25–28]

T cell responses are critical for developing lasting immunity against SARS-CoV-2. Helper T cells contribute to activation and maturation of both B cells and cytotoxic T cells while also producing cytokines that can coordinate both innate and adaptive antiviral immune responses.[29] T cell responses against SARS-CoV-2 antigens reduce disease severity while also improving B cell maturation and production of neutralizing antibodies.[30–32] In individuals previously infected with SARS-CoV-2, T cell responses can be stably detected for over a year.[32] In addition, T cell-mediated responses can target a broader range of epitopes in comparison to antibodies, so mutations that confer resistance to pre-existing immunity are less likely to develop. The S protein, which is the dominant antigen in most vaccines and prominent target of neutralizing antibodies, is subject to significant selective pressure mediated by the immune system; thus immunization strategies focused on S-based immunogens have higher propensity for immune escape. In fact, with new variants such as Omicron, even T cell responses have been found to be less capable of recognizing S epitopes.[3,33] However, SARS-CoV-2 encodes many immunodominant T cell epitopes in other proteins.[34–38] For instance, the nucleocapsid protein (N) is one of the most prominent T cell antigens of all SARS-CoV-2 proteins, and its epitopes are the dominant target of major histocompatibility complex (MHC) class II.[34] The T cell responses against N are also remarkably long-lasting as evident from a recent study showing that individuals infected with SARS-CoV during the original 2003 outbreak still had memory T cells that were cross-reactive against the SARS-CoV-2 N protein.[39] The N protein is also highly conserved among coronaviruses and has significantly fewer mutations in SARS-CoV-2 VOCs compared to S.[40,41]

T cell-targeted immunogens can also be specifically designed by incorporating immunodominant epitopes into a single polypeptide chain—known as a poly-epitope antigen.[42–45] Through extensive screening of COVID-19-positive individuals, many of the immunodominant T cell epitopes of SARS-CoV-2 proteins have been discovered and classified by histocompatibility leukocyte antigen (HLA) restrictions.[34–38] In this study, we strategically designed a poly-epitope antigen using immunodominant epitopes that stimulate both CD4 and CD8 T cells and that are highly conserved across known VOCs. Since epitopes are derived from many proteins, the likelihood of mutations developing that confer resistance against the vaccine can be significantly reduced. Adding to this is the ability to select epitopes in functionally important regions that if mutated could affect the viability of the virion and further reduce the risk of vaccine resistance.

In this study, we develop and test a multi-antigen VACV-based vaccine that encodes regions of S and N in combination with a poly-epitope antigen that includes immunodominant epitopes from seven different SARS-CoV-2 proteins. In creating this vaccine, we also delete two VACV genes that are important for replication and immune modulation and which significantly reduce its toxicity while improving its immunogenicity. The new vaccine, named TOH-VAC-2, generates robust, long-lasting humoral immunity against both S and N antigens and elicits potent T cell responses against S, N, and epitopes within the polyantigen. Heterologous challenge of vaccinated mice with viruses expressing each antigen shows that N is important for providing protective T cell immunity, while expression of the polyantigen stimulates expansion of T cells in the infected tissues. Ultimately, TOH-VAC-2 is a promising vaccine for generating long-lasting protective immunity against the many variants of SARS-CoV-2 and may help to overcome low vaccination rates in countries around the world.

RESULTS

Design and generation of TOH-VAC-2 vaccine

Our previously developed SARS-CoV-2 vaccine, TOH-VAC-1 (TV1), encoded a membrane-tethered version of the RBD (referred herein as

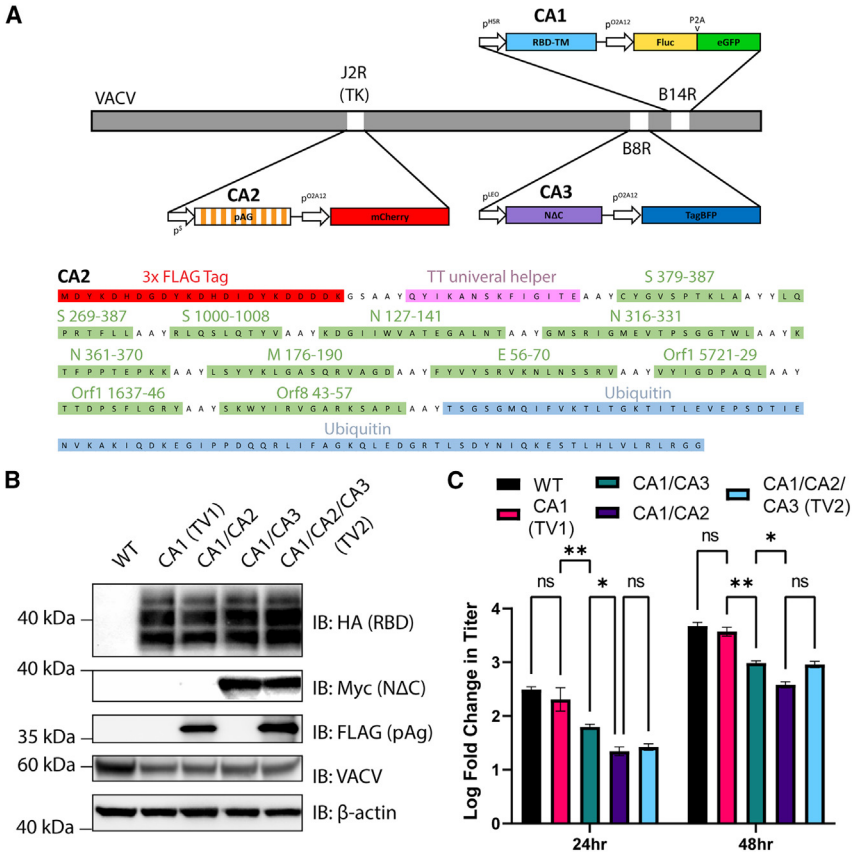

Figure 1. Vaccine design and validation

(A) Schematic diagram of SARS-CoV-2 immunogens and their inserted locations in the vaccinia genome. The primary amino acid sequence of the poly-epitope antigen with indicated peptides from SARS-CoV-2 is provided below. (B) Immunoblot showing expression of vaccine antigens from U2OS cells infected with each vaccine. Cells were infected at an MOI of 0.5 for 24 h. (C) Growth rates of the vaccines in U2OS cells. Growth rate was measured as a fold increase in viral titer from the initial viral PFU used to infect cells (n = 3 technical replicates). Statistical significance was determined via two-way ANOVA with Tukey correction (*$p < 0.0361$; **$p < 0.0021$; ***$p < 0.0002$; ****$p < 0.0001$) (full analysis in Table S3).

CA1) as immunogen.[13] In order to increase SARS-CoV-2-specific responses and to reduce the risk of vaccine resistance resulting from mutations, we introduced two new antigen sequences to TV1 (Figure 1A). For the first antigen, we employed a truncated N lacking the C-terminal dimerization domain (referred herein as CA3). The dimerization domain of N was removed to prevent it from undergoing phase separation, which is linked to decreasing innate antiviral immune responses by increasing activity of the mitochondrial antiviral-signaling protein.[46–48] CA3 was inserted into the VACV genome at the B8R gene locus, which encodes a virulence factor that acts as an interferon-γ (IFNγ) decoy receptor.[49,50] Disrupting B8R enables more efficient IFNγ signaling, which enhances T cell immunity. Additionally, B8R removal should provide a safer platform that is less capable of modulating host immunity.[49,50] However, it is important to note that B8R affinity toward murine IFNγ is substantially lower than human IFNγ, and any benefits from a B8R deletion in mice are expected to be minimal.[49,50]

The second immunogen that was designed for our second-generation COVID-19 vaccine was a polyantigen (referred herein as CA2) created from epitopes from a variety of SARS-CoV-2 proteins to reduce the risk of resistance arising from random mutations. The epitopes were selected based on their ability to elicit strong T cell responses from individuals previously infected with SARS-CoV-2 and to cover a wide range of HLA restrictions, so that it could provide broader coverage of the worldwide population (Figure 1A; Table 1).[34,35] The polyantigen includes several immunodominant epitopes from regions of S and N that are not contained with the CA1 or CA3 antigens. In addition to the SARS-CoV-2 epitopes, the polyantigen contains the sequence for the tetanus toxoid universal helper peptide, which elicits strong T cell responses in both humans and mice with a variety of HLA restrictions and can help boost overall T cell immunity.[45,51–53] A ubiquitin tag was also added at its C terminus as this was shown previously to promote antigen processing and enhance T cell-specific responses against the individual epitopes.[45,54] CA2 was encoded into the J2R gene of VACV—a genetically stable locus that is commonly used to express recombinant genes.[55,56] The disruption of J2R was also intended to attenuate the TT backbone and improve its safety profile since it encodes a thymidine kinase (TK)—an important metabolic protein involved in VACV DNA synthesis. However, unlike MVA, TK-deleted VACV can still grow in many cell lines and to a limited extent *in vivo* by borrowing the TK produced by cells during their own replication.

To examine the potential risk of resistance against the newly designed vaccine antigens, we profiled the frequency and location of mutations within the sequences of RBD, N, and CA2 from major SARS-CoV-2 VOCs. The RBD of the S protein, which is commonly used in SARS-CoV-2 vaccine design, has many variants distributed throughout its sequence (Figure S1A). The Omicron variant alone has 36 different mutations in the S protein, 15 of which are found in the RBD sequence. In contrast, the N protein has substantially fewer mutations, which also are localized more generally around specific regions (Figure S1B). In CA2, out of the 11 epitopes that comprise the polyantigen, there is only a single mutation in one of the epitopes that has been identified in a VOC (Table 1). Hence, the low frequency of mutations in N and the CA2 epitopes exemplifies why they are good candidates for making a variant-resistant COVID-19 vaccine.

Table 1. Antibodies used in intracellular cytokine staining

Target	Fluorophore	Dilution	Company
CD45	FITC	1:100	BD (clone 104)
CD3	Alexa Fluor 700	1:100	BioLegend (Clone 17A2)
CD4	BV786	1:100	BD (clone R4-5)
CD8	PerCP-Cy5.5	1:100	BD (clone 53-6.7)
IFNγ	APC	1:100	Invitrogen (Clone XMG1.2)
TNFα	PE-Cy7	1:100	BioLegend (Clone MP6-XT22)

We generated TT-vectored vaccines that expressed each possible combination of CA2 and CA3 immunogens in combination with the membrane-tethered RBD (i.e., CA1/CA2, CA1/CA3, and CA1/CA2/CA3, also referred to as TOH-VAC-2 or TV2). Expression of the antigens was confirmed by immunoblotting lysates from infected U2OS cells (Figure 1B). Interestingly, the immunoblot against CA2 resulted in a banded ladder, most likely indicative of poly-ubiquitination (Figure S2A). There was also evidence of smaller bands indicating proteolytic degradation. Immunofluorescence also showed that CA2 also localized around the nucleus in the endoplasmic reticulum (Figure S2B). Lastly, we performed plaque assays to measure the growth of these viruses in U2OS cells to determine how the deletions of B8R and TK affected their ability to replicate. Both TK and B8R deletions significantly decreased viral growth relative to wild-type (WT) TT and TT CA1 (also referred to TOH-VAC-1 or TV1) (Figure 1C). The TK$^-$ constructs both led to a 10-fold reduction in viral titers after 24 and 48 h of infection.

Safety profiling of new Tiantan vaccines

The B8R and TK deletions in the new TOH-VAC-2 vaccine were designed to improve safety and immunogenicity relative to the first version of the vaccine. While TV1 had an overall good safety profile when administered to immune-competent mice and non-human primates, it did lead to some side effects, such as weight loss and pox lesions at the injection site.[13] In addition, TV1 exhibited severe cytotoxicity when administered systemically to immune-deficient nude mice.[13] To test the safety of the new attenuated vaccines, we administered the viruses intravenously (i.v.) in nude mice, similar to what we did previously for TV1.[13] The mice were injected with every possible combination of the proposed attenuations—WT, B14R$^-$ (TV1), B14R$^-$/TK$^-$ (CA1/CA2), B14R$^-$/B8R$^-$ (CA1/CA3), and B14R$^-$/B8R$^-$/TK$^-$ (TV2)—and monitored for weight loss, pox lesion development, and visual signs of severe infection (i.e., lethargy, hunched back, respiratory distress, etc.). The mice that received TT WT, TV1, or CA1/CA3 all lost 10%–20% of their body weight and developed severe pox lesions over their body within 7 days of their administration (Figure 2A). Ultimately, due to their rapid weight loss and symptoms of severe poxvirus infection, the mice were all euthanized 7 days after injection (Figure 2B). In contrast, mice injected with TK$^-$ viruses had no significant loss in weight compared to saline-injected mice until after 20 days (Figure 2A). At this point, some mice in the TK$^-$ groups began developing pox lesions and losing weight, which led to their eventual euthanization. However, 40%–60% of the mice in the TK$^-$ groups survived (Figure 2B). IVIS imaging was also used to monitor the distribution of viral replication in nude mice 3 days after injection (Figures 2C and 2D). The TV1 and CA1/CA3 viruses both spread systemically through the mice and caused extensive formation of pox lesions on their tails (20 ± 3 and 25 ± 3 for TV1 and CA1/CA3, respectively) (Figures 2C–2E). Whereas, both TK$^-$ viruses had no detectable luciferase activity anywhere in the mice, and there were only a small number of minor lesions present on their tails (1.4 ± 0.7 and 5.2 ± 1.7 for CA1/CA2 and TV2, respectively). Altogether, this shows that the TK deletion significantly improves the safety of the TT-based vaccine vector.

TOH-VAC-2 induces robust humoral immunity against both RBD and N

We previously showed that TV1 elicited robust, long-lasting neutralizing antibody production with only a single dose of the vaccine.[13] Since TV2 is less effective at replicating both *in vitro* and *in vivo*, we tested whether it could similarly produce high levels of RBD-specific antibodies using only a single dose of the vaccine. The titers of RBD-specific antibodies were measured from mice that received either one or two doses of the vaccines (delivered intranasally 36 days apart) (Figure 3A). The titers of RBD-specific antibodies were as high in the attenuated TV2 vaccine as they were for the non-attenuated TV1 vaccine group. The CA1/CA3 group also had similar levels of RBD antibody production, while the CA1/CA2 appeared to have slightly lower, but not statistically significant, levels. For each vaccine, we also saw no significant difference in RBD antibody titers between mice receiving either one or two doses. RBD antibody titers were measured for up to 90 days post immunization for both single-dose (Figure 3B) and double-dose (Figure S3A) vaccines, and the antibody levels remained relatively consistent over this time with the TV1, CA1/CA3, and TV2 vaccines all providing similar performance. Interestingly, the levels of RBD antibodies for the CA1/CA2 vaccine group was slightly lower for the first ~60 days after immunization but reached similar levels to the other groups by day 90.

We next measured the levels of antibodies directed against the N protein (Figure 3C). It is not well known if N antibodies play a role in SARS-CoV-2 neutralization, but they can play a role in blocking N-induced complement hyperactivation, which increases the risk of mortality in COVID-19 patients,[57] and they can enhance production of inflammatory cytokines such as IL-6.[58] No N-specific antibodies were detected with the CA1 vaccine, and only a small amount of N antibodies were measured for the CA1/CA2 vaccine (likely due to the presence of N epitopes in the polyantigen). However, high levels of N-specific antibodies were detected for both the CA1/CA3 and TV2 vaccines. CA1/CA3 did not exhibit significant differences in the quantity of N-specific antibodies produced from either one or two doses of the vaccine. Whereas, TV2 produced higher levels of N-specific antibodies starting 14 days after the second dose (Figures 3C and 3D). The titers of N antibodies produced from TV2 were slightly lower than those produced from the

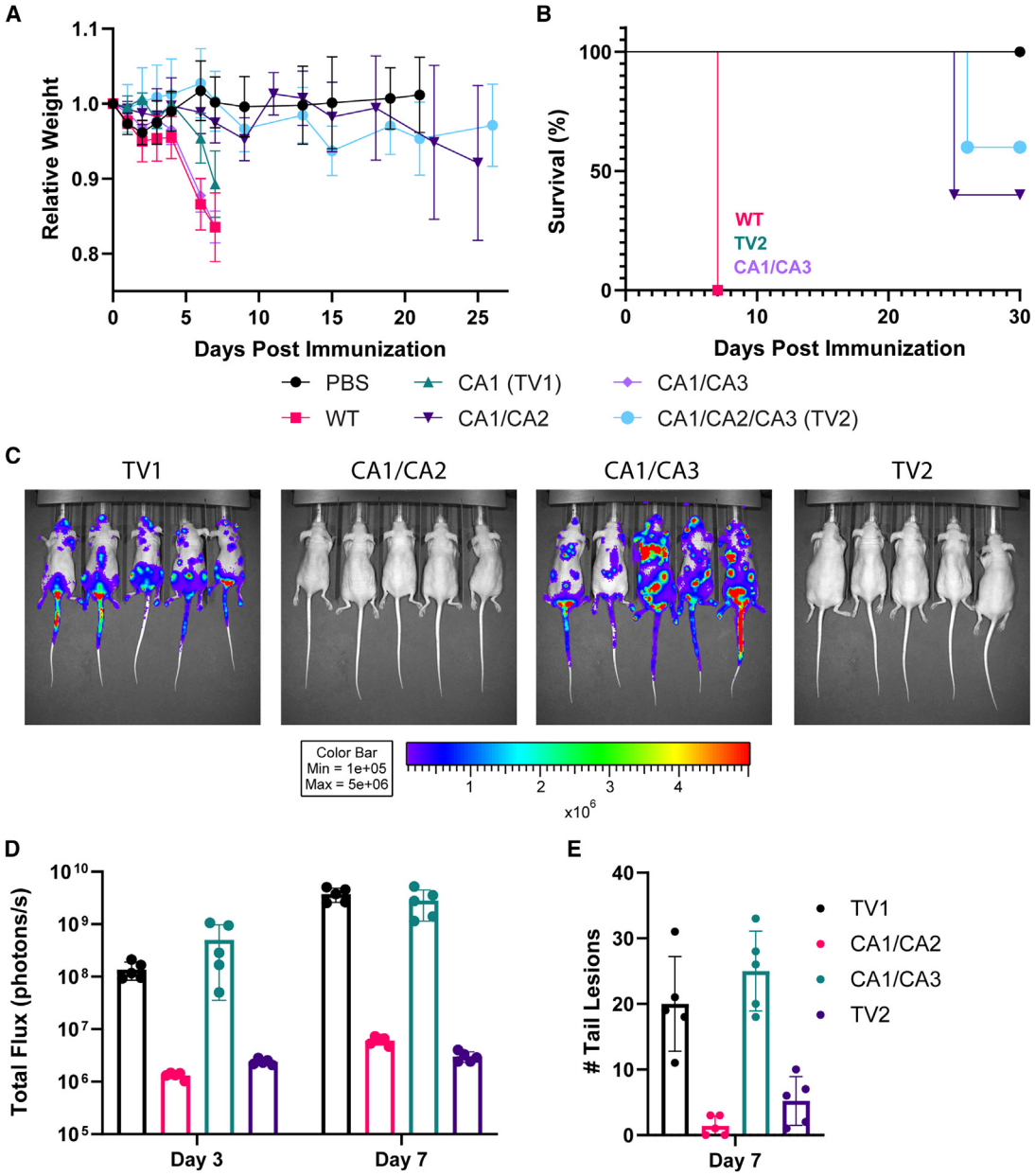

Figure 2. Safety profile of new TT vaccines

(A) Relative change in weight for nude mice infected i.v. with TT viruses at a dose of 1E–6 PFU. (B) Survival rate of mice from (A). (C) IVIS images from nude mice acquired 3 days after infection. (D) Resulting flux measurements from IVIS data in (C). (E) Measurements of pox lesions on the tails of infected mice. Statistical analysis for (D) and (E) is provided in Tables S4 and S5.

non-attenuated CA1/CA3 vaccine, but by day 90 after administering a second dose of TV2, the concentrations were similar to those from CA1/CA3.

Lastly, we analyzed the neutralizing capacity of RBD-specific antibodies against a spike-pseudotyped VSV (Figures 3E and 3F). Each vaccine generated RBD-specific antibodies that were capable of binding VSV-S and preventing infection of Vero-E6 cells. The results from each vaccine also correlated with the levels of RBD antibodies detected by ELISA, with TV1, CA1/CA3, and TOH-VAC-2 having similar IC_{50} values over a period of 90 days, while the CA1/CA2 vaccine was slightly less effective at neutralizing VSV-S. There was also no difference in the neutralizing efficiency between mice receiving one or two doses of the vaccines (Figure S3B). Altogether, the results show that the TK deletion in the TV2 vaccine, which attenuates the virus and significantly

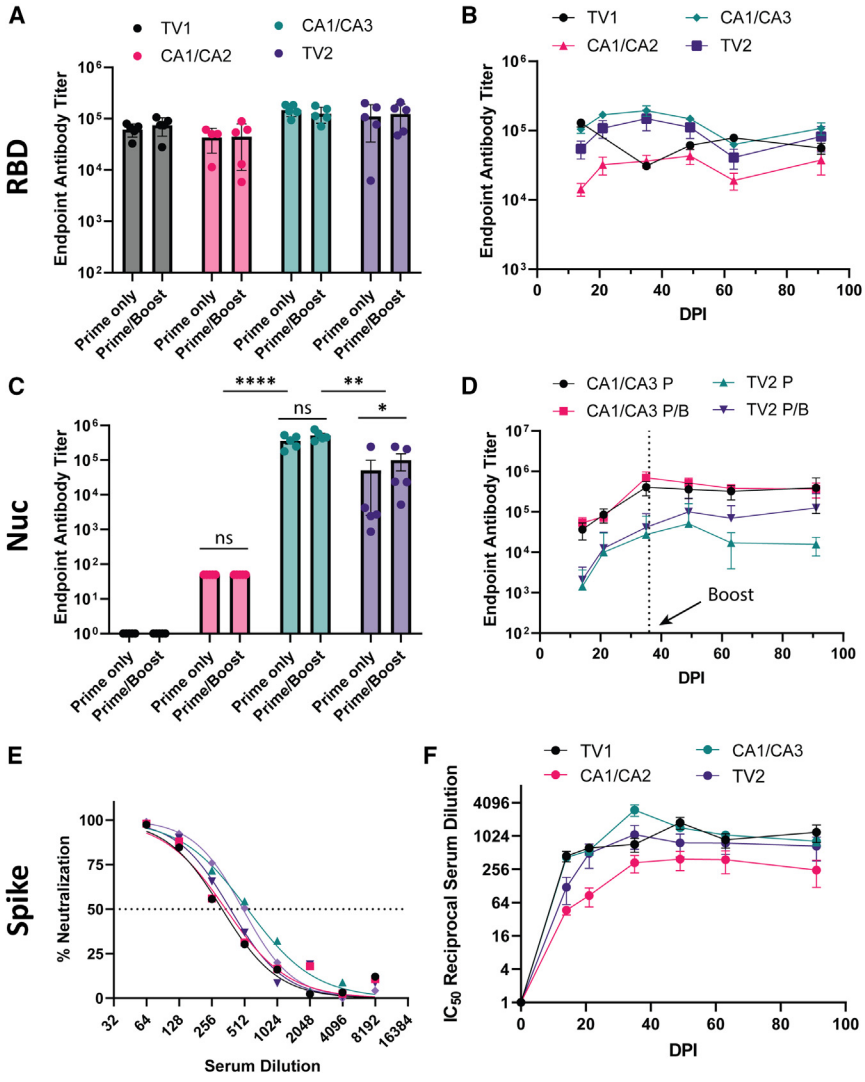

Figure 3. Measurement of RBD and nucleocapsid antibody production and neutralizing titers

(A) Endpoint titers for RBD-specific antibodies in sera of BALB/c mice taken 49 days after intranasal immunization. Mice were boosted intranasally with a second dose of vaccines on day 36. There was no statistical difference between groups (Table S6; n = 5). (B) RBD Antibody endpoint titers for mice receiving only a single dose up to 91 days post immunization (DPI) (prime/boost results are provided in Figure S3). (C) Similar to (A) except for nucleocapsid-specific antibodies. Full statistical analysis is provided in Table S7. (D) Nucleocapsid antibody endpoint titers for mice receiving 1 (P) or 2 (P/B) doses of vaccines up to 91 days post injection (DPI). (E) Representative neutralization curve of VSV-spike with serum from vaccinated mice. (F) The IC_{50} serum dilutions for single doses of each vaccine against VSV-spike up to 90 DPI. Prime/boost neutralization results are provided in Figure S3. Statistical significance for ANOVA analyses in figure is as follows: *p < 0.0361; **p < 0.0021; ***p < 0.0002; ****p < 0.0001.

improves its safety, does not negatively impact antibody development *in vivo*.

TOH-VAC-2 generates robust T cell immunity against SARS-CoV-2 antigens in mice

To examine the T cell responses against the newly designed antigens, we performed IFNγ ELISpot assays with the splenocytes of vaccinated BALB/c mice restimulated *ex vivo* with peptide pools for RBD, N, the polyantigen, and VACV. Each vaccine that expressed CA1 generated strong responses against the RBD peptide pool (Figure 4A). However, CA1/CA3 was significantly lower than the other groups despite being able to replicate efficiently *in vivo* and produce high levels of RBD and N antibodies. Both vaccines that expressed CA2 also had stronger T cell responses against RBD peptides than TV1, despite their attenuation from the TK deletion. In particular, the average RBD response of TV2 (701 ± 144 spot-forming units [SFU]) was almost double that of TV1 (386 ± 87 SFU). TV2 was also the only vaccine capable of producing significant T cell responses against N peptides (Figure 4B). We also found that CA1/CA2 and TV2 were capable of stimulating low, but significant, responses against the epitopes in the polyantigen (not including tetanus toxoid, RBD, or ubiquitin epitopes), despite the epitopes in this construct being designed against human HLA restrictions, which show that the CA2 antigen still displays some immunogenicity in mice (Figure 4C). Furthermore, TV2 elicits strong responses against the tetanus toxoid helper peptide (Figure S4A), which confirms that epitopes within CA2 can undergo proper processing and presentation via MHC. All vaccines generated strong responses against the VACV epitopes, but the B8R^{-} and TK^{-} viruses had reduced responses relative to the non-attenuated WT and CA1 vectors (Figure 4D), which correlates with their reduced rate of replication and cytotoxicity.

For TV2, we also checked if responses could be enhanced further by administering a second dose of the vaccine (15 days apart). Splenocytes were harvested 7 and 14 days after the first dose or 3 and 14 days after the second dose and restimulated with peptides against RBD, N, the polyantigen, or VACV (Figure S4B). We detected significant responses for each peptide pool at each of the time points, but the responses 14 days after the second dose (day 29) were lower than all previous days (although not significantly). The responses for N and polyantigen were similar for days 7, 17, and 18 (3 days post boost), while the response against RBD was slightly higher at the day 7 mark.

To characterize the nature of these T cell responses further, we performed intracellular cytokine staining (ICS) to break down CD4 vs.

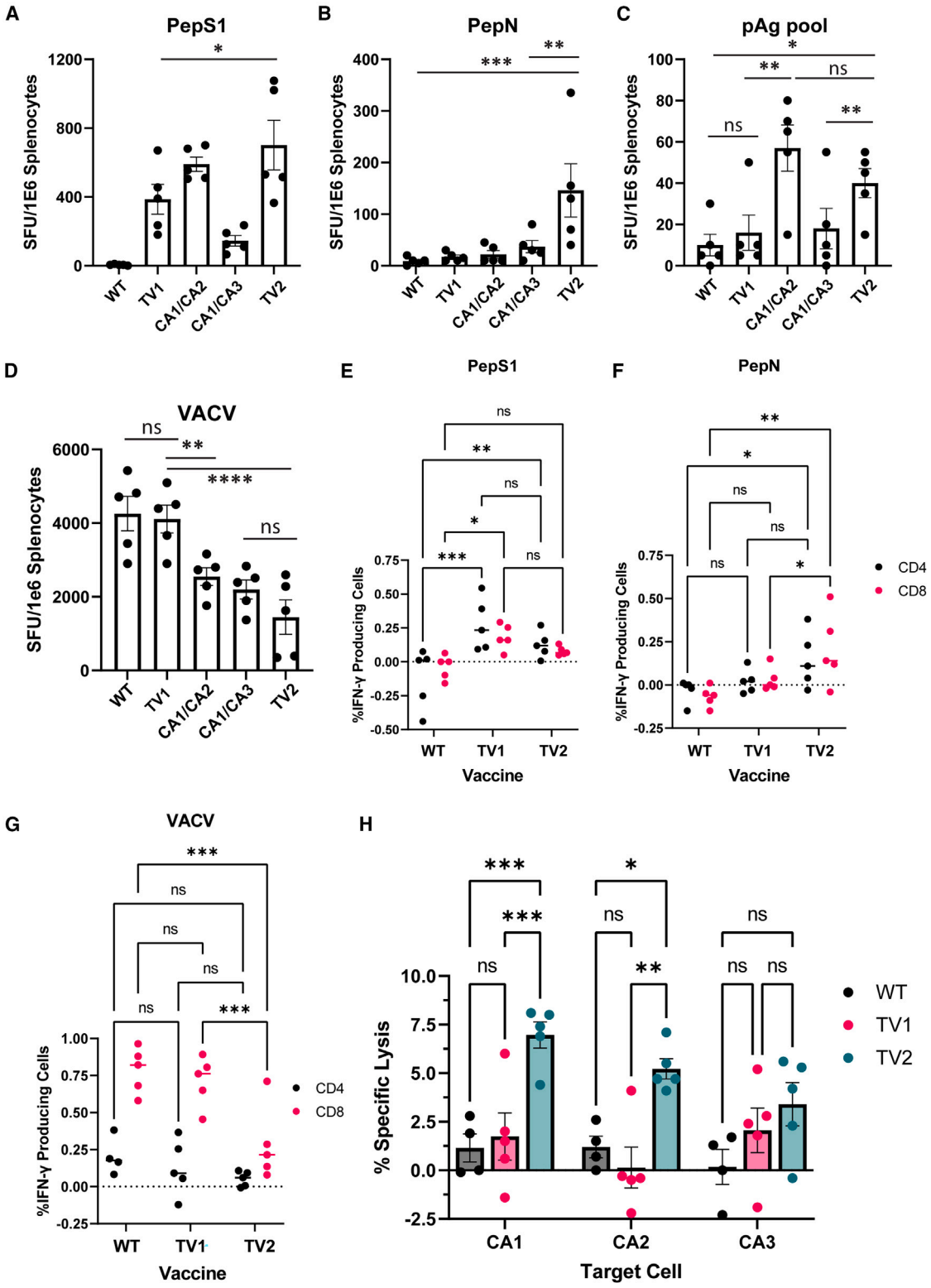

(legend on next page)

CD8 responses against the different SARS-CoV-2 antigens focusing on the new TV2 vaccine and comparing to our initial design (TV1) and the empty vector (WT) (gating protocols shown in Figure S5). For RBD responses, the contribution of IFNγ-producing cells was roughly equal between CD4- and CD8-positive T cell populations (Figure 4E). Both TV1- and TV2-vaccinated groups had significantly higher CD4 responses compared to WT, but there were no significant differences between TV1 and TV2. TV2 was the only group to have a significant response against N, and the response was relatively balanced between CD4 and CD8 populations (Figure 4F). Stimulation with the polyantigen peptide pool was not strong enough in murine sample to stimulate a significant response by ICS in either CD4 or CD8 populations (data not shown). For each vaccine, the response against the immunodominant VACV peptides was predominantly mediated by CD8 T cells (Figure 4G). The responses against VACV peptides were also decreased with the TV2 vector compared to WT and TV1, similarly to ELISpot results.

We next investigated whether the T cell immunity generated by TV2 could provide protection against infection by recognizing and killing cells expressing SARS-CoV-2 antigens. We used lentiviral transduction to generate CT26LacZ cell lines that stably expressed CA1, CA2, or CA3 (Figures S4C–S4F) and co-cultured these cells with T cells isolated from the spleens of vaccinated BALB/c mice. Specific lysis of target cells was then measured by flow cytometry. Interestingly, we detected no significant increase in specific lysis by T cells from TV1-vaccinated mice in comparison to mice receiving empty vector (Figure 4H). In contrast, TV2 vaccination led to a significant increase in the specific killing of cells expressing CA1, CA2, or CA3. Altogether, the results demonstrate the promise of encoding multiple T cell antigens in a COVID-19 vaccine to boost cellular immunity and to provide additional targets to help overcome vaccine-resistant variants.

Polyantigen epitopes elicit strong T cell responses from PBMCs of previously infected individuals

Our ELISpot and co-culture experiments showed that CA2 elicits some level of T cell-mediated immunity in mice despite the epitopes being selected based on responses to human HLA restrictions. However, the response measured against CA2 in mice is substantially lower than those of CA1 and CA3. To determine if CA2 could provide robust T cell immunity in humans, we measured T cell responses against the RBD, N, and CA2 by IFNγ ELISpot for peripheral blood mononuclear cells (PBMCs) from human donors who have previously been infected with SARS-COV-2. The details of their infection and vaccination status are provided in Table S2. All 12 donors responded against the RBD, N, and CA2 peptide pools (Figure 5A). For most donors, the strongest response that was generated was against the RBD pool. In the 10 donors that we collected from, all had received at least two doses of S-based vaccines, while most had only been infected with SARS-CoV-2 once. Donor 9 was the only person to produce a stronger response against a non-S antigen, and they were also the only donor from our list to be infected twice with SARS-CoV-2. Donors 2, SC1, and SC2 all exhibited very strong responses against the CA2 pool. Donor 2 had the briefest collection period between infection and testing of only 2 weeks, while donors SC1 and SC2 both had at least three HLA alleles that matched HLA restrictions of specific peptides. These include HLA-A*2:01 and HLA-DRB1*11:01, which were found in both donors and targeted against S, N, E, and Orf8 epitopes.

To further confirm that the CA1, CA2, and CA3 antigens expressed in our vaccine were immunologically relevant with respect to immunity against SARS-CoV-2, we restimulated PBMCs of previously infected donors with the cell lysates of U2OS cells that were infected with TT WT, TV1, or TV2 (Figure 5B). Most donors had little to no response against the empty vector, and only three of the 10 donors had a response against TV1 that was higher than TT WT. In contrast, eight out of the 10 donors had responses against TV2 that were notably higher than TV1. Altogether, these results show that TV2 can effectively generate T cell responses that are immunologically relevant to humans.

TOH-VAC-2 protects mice against heterologous challenge with VSV viruses expressing COVID antigens

A heterologous challenge model was developed to test the protective potential of each COVID antigen against infection with a pathological virus. We generated VSV viruses that expressed either CA1, CA2, or CA3 (Figure S6) and used them to intranasally challenge either unvaccinated mice or mice immunized with TOH-VAC-2 (Figure 6A). The VSV G protein was not replaced in any of these viruses so that the relative contribution that each antigen makes to eliciting cellular immunity could be dissected. We monitored progression of the illness by measuring the weights of mice after VSV delivery, and 3 days after infection, we collected lungs for titering and histology. With this model, we looked for whether an antigen expressed by TOH-VAC-2 could provide protection against another virus expressing the same antigen. All unvaccinated mice lost 10%–15% body weight after 3 days when administered a VSV virus regardless of COVID antigen (Figure 6B). Vaccinated mice challenged with WT VSV also lost ∼13% body weight, but those challenged with VSV-CA1, CA2, or CA3 only lost 7%, 4%, and 6% body weight, respectively. For CA2, the average difference in percent body weight between vaccinated and unvaccinated groups was ∼10%.

Figure 4. T cell responses against SARS-CoV-2 antigens

(A–D) Results from IFNγ ELISpot with BALB/c splenocytes harvested 7 days after intranasal immunization with TT vaccines (n = 5). Splenocytes were restimulated *ex vivo* using RBD (A), N (B), pAg (C), or VACV (D) specific peptides. (E–G) Intracellular cytokine staining (ICS) of BALB/c splenocytes stimulated with SARS-CoV-2 RBD (PepS1), N (PepN), or VACV peptide pools. (H) Specific killing of CT26LacZ stable cell lines expressing vaccine antigens with T cells isolated from splenocytes of immunized BALB/c mice. T cells were collected 7 days after vaccination. Statistical significance for ANOVA analyses in figure is as follows: *$p < 0.0361$; **$p < 0.0021$; ***$p < 0.0002$; ****$p < 0.0001$.

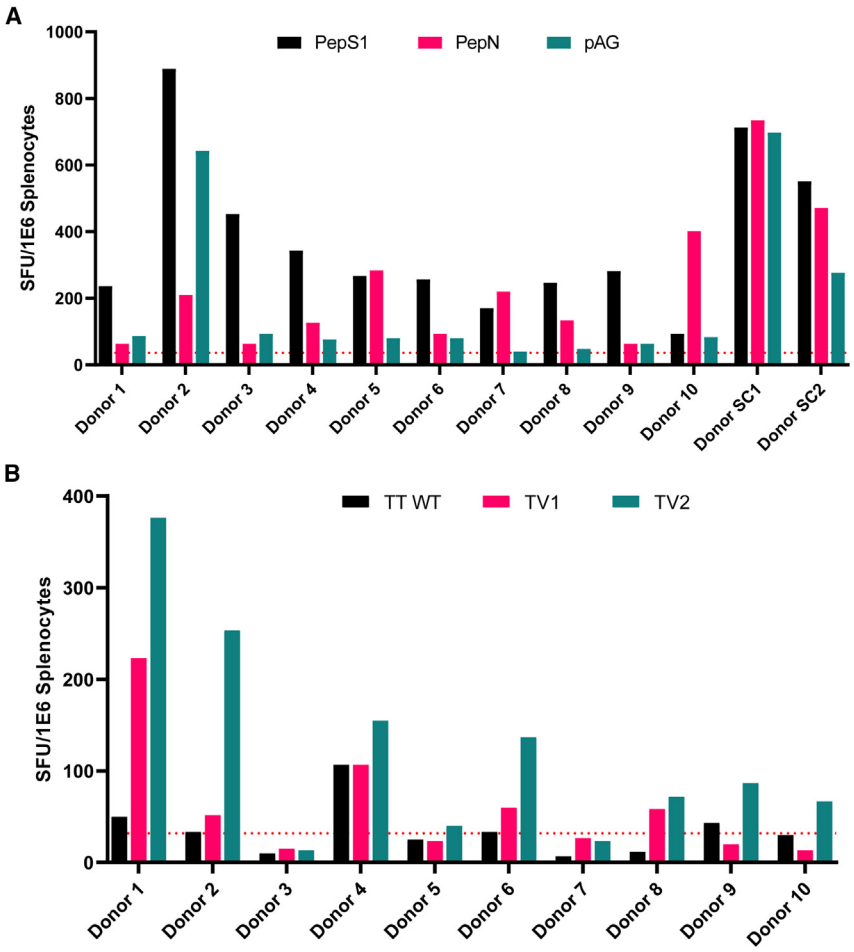

Figure 5. T cell responses against TV2 antigen PBMCs of humans previously infected with COVID-19

(A) IFNγ ELISpot results of human donor PBMCs restimulated *ex vivo* with RBD (PepS1), nucleocapsid (PepN), or CA2 antigen (pAG) peptide pools. The horizontal dashed line indicates the average plus one standard deviation of the negative controls for all donors. (B) IFNγ ELISpot results of human donor PBMCs restimulated *ex vivo* with the lysates of U2OS cells infected with TT WT, TV1, or TV2. Cells were infected at an MOI of 0.3 for 24 h. The horizontal dashed line indicates the average plus one standard deviation of the negative controls for all donors. Donor information is provided in Table S2.

Lungs were removed from infected mice 3 days after infection with VSV, and half of them were homogenized and titered for VSV (Figure 6C). There were no significant differences in the viral titers of lungs from vaccinated vs. unvaccinated mice that were challenged with VSV- WT, CA1, or CA2. However, the titer of VSV CA3 was ~1,000-fold less in vaccinated animals (0.03 ± 0.02 plaque-forming units [PFU]/mg) compared with their unvaccinated counterparts (118 ± 42 PFU/mg). The second half of the lungs were sectioned and stained with a polyclonal VSV antibody (Figure 6D). Similar to the viral titers, we observed no significant differences in the percentage of infected tissue between vaccinated vs. unvaccinated mice for any VSV virus except CA3. In unvaccinated mice, VSV-CA3 was found extensively throughout the lungs for all mice, while in all vaccinated mice, VSV-CA3 was undetectable (Figures 6D and 6E).

Lung sections were also stained for CD4- and CD8-positive T cells to determine if T cells were expanded in the lungs following restimulation with the antigens expressed in a heterologous manner through VSV infection. In unvaccinated mice, there was no significant difference in the number of either CD4- or CD8-positive T cells in lungs of mice infected with any of the VSV viruses (Figures 6F–6I). Whereas, in vaccinated mice, those administered VSV-CA1, CA2, or CA3 saw significant increases in CD4-positive T cells relative to VSV WT (Figure 6H). Interestingly, the virus that caused the biggest increase in the number of CD4 T cells was VSV-CA2 (Figures 6F and 6H). It also appeared that CD4-positive T cell levels in VSV WT administered mice were higher in the vaccinated mice compared to the unvaccinated. This may be explained by mice having higher levels of T cells from the intranasal immunization with TOH-VAC-2, which occurred only 14 days before challenge with VSV. The CD8-positive T cell levels displayed a similar trend to the CD4 analysis with the VSV-CA2 group also seeing the largest increase in the number of CD8 T cells (Figures 6G and 6I). CD8-positive T cells were also increased in lungs of vaccinated mice infected with VSV-CA1 and VSV-CA3 (although not significantly for CA3). Altogether, the vaccination of mice with TOH-VAC-2 provides protective immunity against heterologous challenge with a virus expressing SARS-CoV-2 antigens, through the generation of robust T cell-driven immune responses.

DISCUSSION

In this study, we describe our second-generation poxvirus vector-based COVID-19 vaccine, TOH-VAC-2, encoded with modified versions of the RBD and N proteins as well as a novel polyantigen that contains immunodominant epitopes from seven different SARS-CoV-2 proteins. The new vaccine incorporates deletions at the TK (J2R) and B8R loci in VACV, which improve the safety profile of the vaccine without compromising the strength or longevity of the immune responses it generates. The TK deletion, in particular, significantly improved survival in immune-deficient mice that were administered virus systemically. TK is an enzyme involved in synthesis of nucleotides that are needed for viral DNA replication. Healthy cells also express TK during replication, but it is rapidly degraded following mitosis, and its levels in the cytoplasm are not sufficient to support VACV replication.[56,59] Hence, viruses with deleted TK

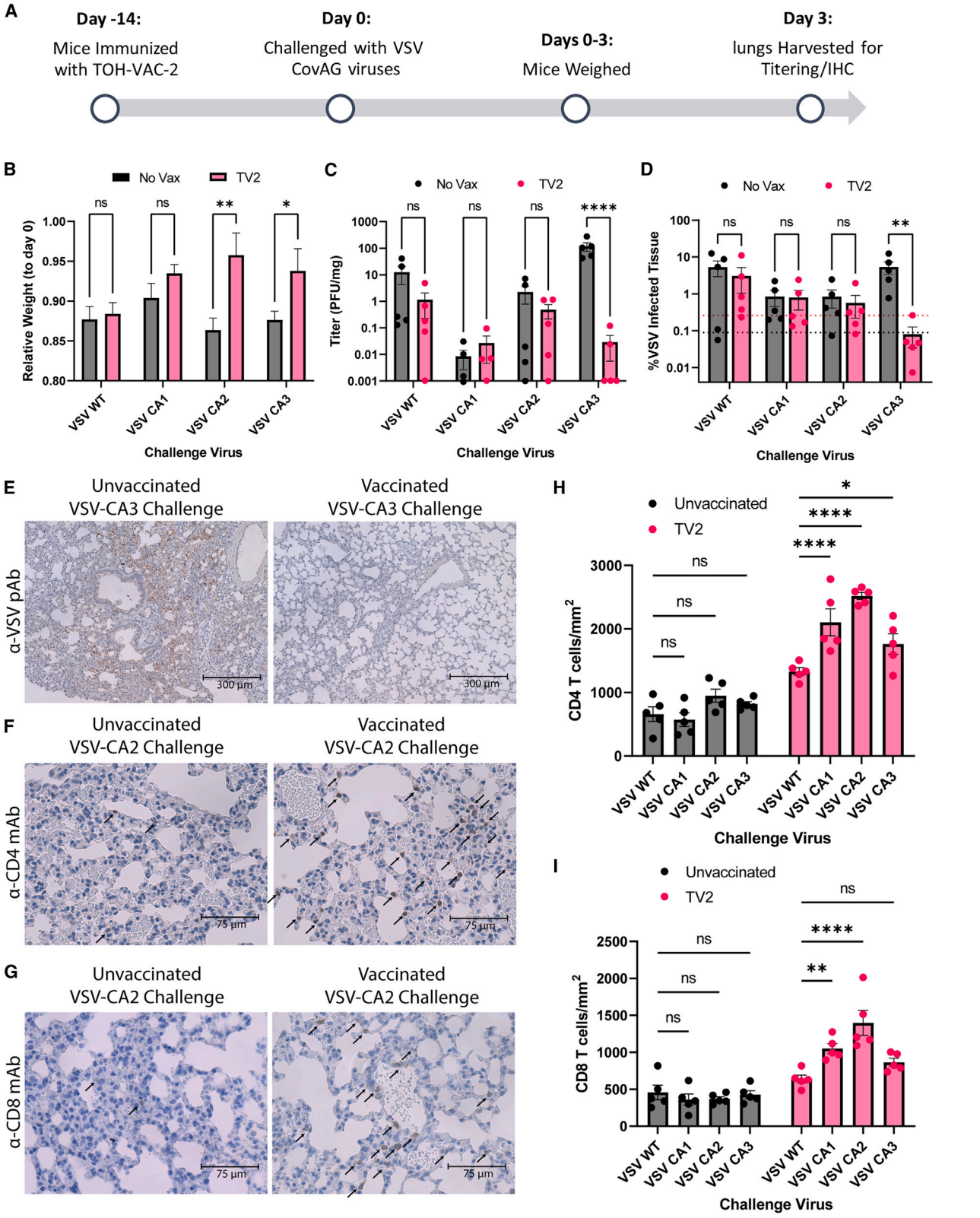

(legend on next page)

genes have decreased virulence *in vivo*.[55,56] However, VACV TK knockouts grow well in cell culture,[60] which make them easy to manufacture in comparison to non-replicating poxvirus vectors such as MVA, which require specialized cell lines to culture.[61,62] We also demonstrated in our prior work that the non-replicating MVA-based vaccine was less effective at generating long-lasting humoral and cellular immunity than the corresponding replicating Tiantan vaccine.[13] TK is also a genetically stable site that has been used regularly to integrate foreign transgenes. However, despite extensive use of TK knockout VACV viruses in the field of oncolytic virotherapy, their use in vaccine development against infectious diseases is rather limited.[56] Here, we show that a TK knockout Tiantan virus generates robust humoral and cellular immunity, similar to its non-attenuated counterpart, while also significantly improving its safety.

The new TOH-VAC-2 vaccine also provides broader protection in contrast to our first generation vaccine (TOH-VAC-1) by incorporating two new antigens: the N-terminal half of the nucleocapsid protein and a polyantigen composed of epitopes from various SARS-CoV-2 proteins. As shown here and in our previous study, the RBD antigen generates robust neutralizing antibodies that provide protection against infection,[13] but as seen from our heterologous challenge experiment, the RBD is not as effective for providing cellular immunity and protecting mice from infection with VSV expressing RBD. In addition, the RBD/spike protein is more prone to mutations that confer resistance to vaccines that use the original Wuhan sequence. In contrast, the N antigen, which is highly conserved among current VOCs, significantly reduces virus infection in the lungs of mice challenged with VSV-N. TOH-VAC-2 also generates high quantities of N-specific antibodies, which are believed to improve therapeutic outcome by blocking N-induced complement hyperactivation that leads to inflammatory lung damage.[57,63,64] The N protein is an ideal candidate to include in SARS-CoV-2 vaccines. Its high sequence conservation among coronaviruses leads to cross-reactive immune responses, and its genetic stability and low occurrence of mutations reduce the risk of vaccine resistance.[39,40] It also generates robust humoral and cellular immunity, which is why many vaccines are now investigating it as antigen to use independently or in conjunction with S.[59,65–70]

We also describe here a unique poly-epitope antigen, CA2, designed with immunodominant T cell epitopes from S, N, E, M, Orf1a, and Orf8. The epitopes were selected based on previous screening of peptides that restimulated T cell-induced IFNγ production in patients who had recovered from COVID-19.[34,35] We further confirmed the immunogenicity of these epitopes by restimulating PBMCs of individuals formerly infected with SARS-CoV-2 *ex vivo* with a CA2 peptide pool and found that nearly all donors responded against the CA2 epitopes. For several individuals, the response against the CA2 pool surpassed that of N and, in some cases, was similar to that of S, despite most individuals receiving multiple doses of S-based vaccines. We also found that CA2 could generate antigen-specific T cell responses in mice despite CA2 epitopes being selected based on their immunogenicity in humans. Mutations in the selected CA2 epitopes are also uncommon among SARS-CoV-2 VOCs, so it complements the CA1 and CA3 antigens in offering protection against a broader range of SARS-CoV-2 targets. The CA2 antigen also helps boost overall T cell immunity. ELISpot responses against the CA1 and CA3 antigens were improved for vaccines that also expressed CA2. In addition, mice vaccinated with TOH-VAC-2 had the largest expansion of CD4- and CD8-positive T cells in their lungs when infected with VSV-CA2. The reason for this could be due to the tetanus toxoid universal helper (TTH) peptide—a universally immunogenic T cell epitope that promiscuously binds to a wide range of MHC class II haplotypes,[51,52,71] and which we found generated strong responses by ELISpot in TOH-VAC-2-immunized mice. Several studies have shown that the TTH peptide can act as a general adjuvant that boosts T cell-specific responses against other antigens in their vaccines.[45,72]

Poly-epitope antigens, such as the one described here, provide an effective strategy for selectively generating T cell responses against specific pathogens or diseases.[42–44] Since epitopes can be selected from various viral antigens, they can provide a broader coverage of viral variants/strains with a reduced likelihood of vaccine resistance. They can also be used to mount immunological responses against specific immunodominant antigens, without encoding regions of those antigens that trigger adverse effects.[44] We have capitalized on this feature by including epitopes from the C-terminal dimerization domain of N, which are potent epitopes of MHC class II,[34] without expressing the full domain, which can suppress innate antiviral immune responses.[46–48] Similarly, we could also avoid potential adverse effects from encoding the full length sequence of S, which is associated with a variety of health complications,[73] such as antibody-dependent enhancement of SARS-CoV-2 infection, which is linked to antibody interactions with the N-terminal domain,[74] as well as a variety of cardiovascular complications, such as myocarditis, which are associated with S2-induced syncytia formation.[75,76] Replicating viral vectors, such as the TT J2R$^-$/B8R$^-$/B14R$^-$ virus used here, provide an ideal delivery platform for poly-epitope antigens. They express the poly-epitope antigen within cells while simultaneously boosting cellular immunity by serving as a potent T cell adjuvant.

Figure 6. Vaccine-induced protection against heterologous challenge with VSV viruses expressing COVID-19 antigens

(A) Schematic timeline of *in vivo* heterologous challenge experiment performed in BALB/c mice (n = 5). (B) Relative loss of weight in mice challenged intranasally with VSV viruses (3 days after infection) 14 days after intranasal vaccination with TV2. (C) VSV titers in the lungs of infected mice harvested 3 days after infection and normalized to the weight of the tissue. (D and E) IHC staining of lung sections from VSV-infected mice using polyclonal VSV antibody. (D) shows the percentage of infected tissue in vaccinated and unvaccinated mice. (E) Representative images of stained lung sections from unvaccinated vs. vaccinated mice challenged with VSV-CA3. (F and G) IHC staining of lung sections from VSV-infected mice using CD4 (F) or CD8 (G) antibodies. Arrows highlight T cells within the tissue. (H and I) The resulting quantification of CD4 (H) and CD8 (I) T cells in the lungs of mice following VSV challenge. Statistical significance for ANOVA analyses in figure is as follows: *$p < 0.0361$; **$p < 0.0021$; ***$p < 0.0002$; ****$p < 0.0001$.

New variants of SARS-CoV-2 continue to emerge with increasing resistance against the immunity provided by vaccines using only the S antigen. The use of seasonal COVID-19 boosters is now being debated for providing continued protection against emerging SARS-CoV-2 VOCs, but with rapid rates of mutation in S, the relatively slow process required for testing and approval of new vaccines, and the rising rates of COVID-19 vaccine hesitancy, the world needs novel vaccines that can provide more durable, mutation-resistant immunity.[11,77–79] Important for this process is the targeting of antigens and epitopes that are highly conserved, unlikely to mutate, and capable of generating potent immunological memory. T cell antigens are important for achieving this goal as they are not limited to extracellular proteins with surface-exposed epitopes that are not necessarily essential for function and thereby prone to mutation. Cellular immunity is important for reducing SARS-CoV-2 replication and decreasing disease severity,[11,30–32] and T cell responses against SARS-CoV-2 antigens are remarkably long-lasting.[32,39] This is why Pfizer and BioNTech are currently pursuing development of BNT162b4, a T cell-directed COVID-19 vaccine that incorporates S, N, M, and parts of ORF1a[67] to enhance the breadth and durability of protection against SARS-CoV-2 and its variants. In this study, we show that our second-generation COVID-19 vaccine, TOH-VAC-2, elicits potent T cell responses in both mice and humans against a variety of SARS-CoV-2 antigens. Furthermore, we show that this cellular immunity provided protection against a completely different virus expressing each of the different antigens that were part of the vaccine. Altogether, TOH-VAC-2 represents a promising vaccine candidate that could be easily manufactured, distributed, and administered to provide robust humoral and cellular immunity against SARS-CoV-2 infections.

MATERIALS AND METHODS

Cell lines and viruses

All cell lines were purchased from the American Type Culture Collections (Manassas, VA) and cultured in Dulbecco's Modified Eagle Medium (DMEM) with 10% FBS. VSV-S/GFP was a kind gift from Dr. Sean Whelan (Washington University School of Medicine).[80] The vaccinia Tiantan strain was a gift from Dr. David Evans.[81] The WT Indiana serotype of VSV used in this study was described previously.[82]

Construct design

The CA1 construct consists of the RBD of the SARS-CoV-2 spike protein (amino acid residues 331–524) fused to its transmembrane (TM) domain (residues 1,208–1,270) via a 3x GGGGS linker (the accession number used for spike sequences is MW070087.1). Upstream of the RBD coding sequence is a murine IL-12 signal peptide followed by a GGSGGG linker. At the C-terminal end of the TM region is an HA-Tag for convenient detection. The RBD-TM construct is expressed by the vaccinia early/late H5R promoter (GenBank: LR877630.1). For recombinant virus selection and tracking of viral growth, genes encoding firefly luciferase and eGFP were incorporated under a separate early/late promoter (composed of O2L and A12L promoters) separated by a P2A sequence. The entire construct noted above was flanked by homology arms for B13R and B14R loci in vaccinia.

The CA2 construct is described in Figure 1A and Table S1. The DNA sequence of the CA2 antigen was created from the amino acid template using codon optimization charts for *homo sapiens*. The VACV pS promoter was added upstream of the construct, and mCherry was added downstream under an early/late promoter (composed of O2L and A12L promoters) as a positive selection marker for purifying the recombinant virus. The entire construct was surrounded by 500-bp homology arms targeting the J2R (TK) locus. Insertion of the construct in the TK locus interrupts the TK gene, resulting in a truncated and non-functional transcript.

CA3 was designed with residues 1–240 of the N protein (GenBank: UAJ55448.1), with an N-terminal 3X Myc tag. The DNA sequence was codon optimized for *homo sapiens*. The construct was under control of the LEO VACV promoter. TagBFP was also included, expressed with the O2L/A12L as a recombinant marker for positive selection. The entire construct was surrounded with homology arms to insert at the B8R gene locus and disrupt the B8R gene function.

Plaque assay

U2OS cells were infected in a six-well plate with TT at an MOI of 0.1 in 1 mL of serum-free DMEM media. After 24 and 48 h, the cells in the wells were scraped from the plate and freeze-thawed at −80°C. The lysates from freeze-thawed samples were serially diluted from 1:100 to 1:1E–9 and added to uninfected U2OS cells. After 2 h of incubation at 37°C, the diluted lysates were removed, and a 1.5% carboxymethylcellulose (CMC) overlay was added to the cells. Cells were then incubated for 48 h at 37°C. TT plaques were detected via crystal violet staining. Titers were normalized to the initial PFU of virus from samples prepared identically at the time of infection, but immediately frozen instead of added to cells.

Mouse experiments

5- to 8-week-old female BALB/c or nude mice (The Jackson Laboratory, Bar Harbor, ME) were obtained for studies. All experiments were approved by the University of Ottawa animal care and veterinary services (MEe-2258-R5 or OHRIe-3340-A), including periodic blood collection using the lateral saphenous vein for serum. Unless noted otherwise, mice were vaccinated intranasally with 1E–6 PFU of TT vaccines.

Safety profiling of TT vaccines

6-week-old BALB/c nude mice were injected i.v. through the tail vein with 1E–6 PFU of TT viruses. The weights of the mice were measured at regular intervals, and they were monitored for pox lesions, respiratory distress, pallor, and fatigue for signs of severe infection. Once mice lost 10%–20% of their body weight and developed severe pox lesions, they were euthanized. *In vivo* luminescence imaging was performed 3 days after infection with an IVIS Spectrum In Vivo Imaging System, as described previously.[13] Mice were injected intraperitoneally with

250 μg of D-luciferin (Invitrogen) dissolved in PBS and rested 5 min prior to imaging.

ELISA

Nunc Maxisorp 96-well flat-bottom plates were coated overnight at 4°C with 125 ng of RBD (prepared in house[11]) or N per well. The following day, the coating solution was removed, and the plates were washed three times with PBS-Tween (0.1% Tween 20) and blocked with 3% skim milk solution for 1 h. Mouse sera from vaccinated mice were then serially diluted in 1% skim milk and added to the plates to incubate for 2 h at room temperature. In addition, a positive and negative control was added to each plate composed of a monoclonal RBD antibody (1 μg/mL; Cat No: MBS434247, Anti-RBD Domain [SARS-CoV-2 spike], monoclonal antibody, MyBioSource, CA, USA) or monoclonal N antibody (1.5 μg/mL; Catalog # MA5-35943, clone 6H3, Thermo), and a pool of sera was taken from mice prior to vaccination. Following the 2-h incubation, plates were washed with PBS-Tween and incubated with anti-mouse IgG conjugated to HRP (1:3,000; Cat No: 314930, Goat anti-Mouse IgG [H + L] Secondary Antibody, HRP, Invitrogen) for 1 h at room temp. Plates were then developed using SigmaFast OPD solution and measured at 490 nm using a Biotek microplate reader.

All experimental absorbance readings were normalized relative to the blank and the positive control (monoclonal RBD antibody at 1 μg/mL) and fit using a quadratic binding polynomial assuming 1:1 binding. The fitting was performed using a Monte Carlo simulation with the non-linear curve fitting tool in QtGrace. The reciprocal antibody titer was determined by interpolating the dilution factor that intersected with a minimum detection threshold defined by 10x the standard deviation of the responses from mice vaccinated with Tiantan WT or to a fixed value of 0.025 (whichever was larger).

ELISpot assays

BALB/c mice were inoculated intranasally with 1E–6 PFU Tiantan vaccines. 7 days after injection, mice were sacrificed, and spleens were harvested for IFN-γ ELISpot assays. Splenocytes were isolated and incubated at a density of 2E–5 cells/well on murine IFN-γ Single-Color ELISpot plates (ImmunoSpot) with either 0.5 μM of PepTivator SARS-CoV-2 Prot S1 pool (Miltenyi Biotec), 500 nM of PepTivator SARS-CoV-2 Prot N pool (Miltenyi Biotec), 5 μM each of VACV F2/E3 peptides (SPGAAGYDL/VGPSNSPTF; Genscript),[83] or 0.2% DMSO. For polyantigen pool, 2 μM of each peptide from Table S1/Figure 1A (synthesized by Genscript) was combined, with exception of the CYGVSPTK peptide, which responds against the RBD antigen (CA1) vaccines. Splenocytes were stimulated with peptides for 20 h, and then the ELISpot was performed according to the manufacturer's protocol. Plates were imaged and spots were counted using an ImmunoSpot Analyzer.

Pseudotyped virus neutralization assay

Vero E6 cells were seeded in 96-well plates such that there were 40,000 cells per well at the time of infection. Serum was first diluted in a separate 96-well plate at a 1:10 dilution in serum-free DMEM, and a serial 1 in 2 dilution series was performed. VSV pseudotyped with the SARS-CoV-2 spike glycoprotein[74] and co-encoded with eGFP was then added to the serum in an equal volume of serum-free DMEM for a final dilution of 2,000 PFU per well and incubated for 1 h at 37°C. After 1 h, medium on the cell was replaced with 60 μL of the virus/serum and incubated for 1 h at 37°C. Wells were then topped up with CMC in DMEM (supplemented with 10% FBS) for a final concentration of 3% CMC and incubated 24 h at 34°C. GFP foci were imaged and counted using a Cellomics ArrayScan VTI HCS Reader.

Intracellular cytokine staining

Spleens were collected from mice 7 days after vaccination, homogenized, passed through a 70-μm nylon mesh, and mixed with ACK lysis buffer (Gibco) to lyse red blood cells. Splenocytes were then resuspended in RPMI media with 10% heat-inactivated FBS and 100 U/ml penicillin/streptomycin (Fisher Scientific). 2E–6 cells were added to a non-treated U-bottom 96-well plate and co-incubated with either 500 nM of PepTivator SARS-CoV-2 Prot S1 pool (Miltenyi Biotec), 500 nM of PepTivator SARS-CoV-2 Prot N pool (Miltenyi Biotec), 5 μM each of VACV F2/E3 peptides (SPGAAGYDL/VGPSNSPTF; Genscript),[83] or 0.2% DMSO. After 4 h of incubation at 37°C, Brefeldin A (Invitrogen) was added to block cytokine release from the Golgi apparatus, and the splenocytes were co-incubated with the peptides for an additional 16 h at 37°C. CD16/CD32 antibodies (553142; BD) were then added to block Fc receptors followed by staining with Fixable Viability stain 510 (BD). Cells were then stained with antibodies against extracellular receptors (detailed in Table 1) in PBS with 0.5% BSA. Cells were fixed and permeabilized with the BD Cytofix/Cytoperm kit (Cat No. 554714) and then stained with antibodies against IFNγ and TNFα (detailed in Table 1). Since TNFα was undetected in the samples, it was not discussed throughout the results. After staining, cells were resuspended in 1% PFA in PBS and analyzed at the University of Ottawa's Flow Cytometry Core Facility or Ottawa Hospital Research Institute Core facility using the BD LSR Fortessa (BD) Flow Cytometers. Analysis of flow data was conducted using FlowJo v10 (FlowJo, Ashland, OR). The gating protocol is shown in Figure S5.

Generation of CT26LacZ stable cell lines

The CA1, CA2, and CA3 constructs were cloned into a pLenti-CMV plasmid with puromycin resistance gene between XbaI and SalI restriction sites. The pLenti vectors were co-transfected into HEK293x cells with psSPAX2 and pMD2.G plasmids at a ratio of 3:2:1, respectively. Transfections were performed in Opti-MEM medium with lipofectamine 2000 transfection reagent. After 4 h, the medium was replaced with DMEM medium with 10% heat-inactivated FBS and 1x Pen/Strep. Cells were then incubated for 48 h at 37°C before collecting and filtering lysates through a 0.45-μm PES filter. Lentivirus fractions were then stored at −80°C. To generate CT26LacZ stable cell lines, the cells were first detached with trypsin and resuspended in DMEM media with 10% heat-inactivated FBS and 10 μg/mL polybrene. The lentivirus was also prepared in DMEM media with 10% heat-inactivated FBS and 10 μg/mL polybrene. 1E–5 cells were then mixed with

lentivirus in 6-well plates and incubated for around 48 h. When cells reached ~80% confluency, puromycin was added at a concentration of 5 μg/mL to select for transduced cell populations. CA1, CA2, and CA3 expression was then probed by western blot as described above.

T cell killing assays

The generation of CT26LacZ stable cell lines expressing CA1, CA2, or CA3 is described in the supplemental information. On the day of the co-culture experiment, the CT26LacZ cells were stained with CFSE (C34554; Thermo) per the manufacturer's instructions to identify them as the target cell population. BALB/c mice were vaccinated intranasally with 1E–6 PFU of the TT vaccines. 7 days after immunization, splenocytes were isolated as described in the ICS section, and CD3-positive T cells were purified using an EasySep Mouse T cell Isolation Kit (StemCell Technologies). 3E–5 CT26LacZ cells were co-cultured with 1.5E–6 T cells (E:T of 1:5) for 6 h at 37°C. Cells were then stained with Horizon Fixable Viability stain 780 (BD) and fixed in 1% PFA in PBS. Samples were analyzed on a BD LSR Fortessa. Cells were first gated with FSC and SSC to identify signal cell populations, followed by CSFE to identify target CT26LacZ cells. Viability was then measured via fixable stain. The viability percentage of CT26LacZ cells that were not co-cultured with T cells was subtracted from the viable percentage of co-cultured cells to calculate the percentage of specific lysis. The experiment was done with five biological replicates.

Human PBMC ELISpot

All blood collection from human donors was approved by the Ottawa Health Science Network Research Ethics Board. Blood was collected in heparin-coated tubes, and PBMCs were isolated by Ficoll density gradient centrifugation. PBMCs were aliquoted and frozen in 90% FBS and 10% DMSO prior to use. In addition, frozen PBMCs for two donors (SC1 and SC2) were acquired from STEMCELL Technologies (Donor ID 888637185 and CE0007739, respectively). ELISpot experiments were performed with IFN-γ Single-Color ELISpot plates (ImmunoSpot) using 3E–5 PBMCs restimulated *ex vivo* with either 500 nM of PepTivator SARS-CoV-2 Prot S1 pool (Miltenyi Biotec), 500 nM of PepTivator SARS-CoV-2 Prot N pool (Miltenyi Biotec), 2.5 μM each of CA2 peptides (as depicted in Figure 1A; Table S1; synthesized by Genscript), 5 μM each of VACV F2/E3 peptides (SPGAAGYDL/VGPSNSPTF; Genscript), or 0.4% DMSO. For TT lysates, U2OS cells were infected in serum-free RPMI media with TT WT, TV1, or TV2 at an MOI of 0.5 for 24 h. Cells were then scraped and freeze-thawed two times to release cytosolic antigens. Cellular debris was then removed by centrifuging at 500 x *g* for 10 min and passing the lysates through a 0.1-μm filter to remove VACV. ELISpot was performed as described by the manufacturer (ImmunoSpot). Plates were imaged, and spots were counted using a CTL ImmunoSpot Analyzer.

Generation of recombinant VSV viruses expressing CA1, CA2, or CA3

The CA1, CA2, and CA3 constructs were cloned between the M and G genes of the VSV genome in a pCS3 vector using the restriction enzymes MluI and AvrII. To rescue the VSV-CA1, CA2, and CA3 viruses, HEK-293T cells were plated at 1E–6 cells/well in six-well plates. 24 h later, the cells were infected with vaccinia virus expressing the T7 polymerase at MOI = 3. After 1.5 h, vaccinia virus was removed, and cells were co-transfected with the plasmids encoding VSV proteins (P, N, L) and the corresponding VSV recombinant backbone using 2 μl of Lipofectamine 2000 per manufacturer's instructions. After 48 h, the medium was collected and used to infect Vero cells (1.5E–6 cells/well). The supernatants were collected 24 h later and filtered (0.2 μm) to remove vaccinia virus. Recombinant viruses were subjected to three rounds of plaque purification on Vero cells followed by validation of transgene expression prior to production scale-up.

Heterologous VSV challenge experiments

Generation of VSV- CA1, CA2, and CA3 is described in the supplemental information. 5-week old BALB/c mice were immunized intranasally with 1E–6 PFU of TOH-VAC-2. After 14 days, vaccinated or similarly aged naive mice were challenged with VSV viruses administered intranasally at a dose of 1E–8 PFU. Weights were monitored before and after infection. 3 days after injection, the lungs of challenged mice were collected and halved. One-half of them were weighed, homogenized, and used for titering VSV on Vero cells by plaque assay, while the second half was fixed in formalin, embedded in paraffin, and sectioned into 4-μm slices for immunohistochemistry staining.

Immunohistochemistry

Paraffin-embedded lung sections were rehydrated in xylenes followed by consecutive washes in 100%, 95%, and 80% ethanol. Antigen retrieval was performed in a 10 mM sodium citrate buffer (pH 6) by heating in a pressure cooker for 10 min. Slides were then incubated in 3% H_2O_2 to block peroxidases and then blocked with 1.5% BSA for 1 h. VSV detection was performed using a rabbit polyclonal VSV antibody, developed previously in house,[84] at a dilution of 1:5,000. CD4- and CD8-positive T cells were detected with α-CD4 (clone D7D2Z, NEB) and α-CD8 (clone D4W2Z; NEB) antibodies at dilutions of 1:100 and 1:400, respectively. Primary antibodies were detected with ImmPRESS horse anti-rabbit IgG polymer kit (Biolynx) and developed with DAB. Slides were imaged with a Zeiss AxioScan Z1, and image analysis was performed in ImageJ.

Statistical analyses

All statistical analyses were performed in GraphPad Prism using one-way or two-way ANOVA (as indicated in figure/table captions). Statistical significance for ANOVA analyses in figures is as follows: *$p < 0.0361$; **$p < 0.0021$; ***$p < 0.0002$; ****$p < 0.0001$. Statistics tables for figures are provided in supplemental information (Tables S3–S12).

Experimental details for VACV growth curve, western blots, and immunofluorescence were described previously[13] and are summarized for this work in the supplemental information.

DATA AND CODE AVAILABILITY

All relevant data can be found in main text and supplemental information. Raw data are available upon request by contacting Stephen Boulton at sboulton@ohri.ca.

SUPPLEMENTAL INFORMATION

Supplemental information can be found online at https://doi.org/10.1016/j.omtm.2023.101110.

ACKNOWLEDGMENTS

The authors disclosed receipt of the following financial support for the research, authorship, and/or publication of this article: this work was possible by the generous support from the Ottawa Hospital Foundation, the Thistledown Foundation, the Terry Fox Research Institute, and the Canadian Cancer Society. This work was also funded by a FastGrant for COVID-19 Science to C.S.I. and J.C.B. and a grant from the Canadian Institutes of Health Research (#448323) to J.C.B. and C.S.I. S.B., T.A., and M.J.F.C. are funded by MITACS Accelerate. Z.T. is funded by NSERC CGS-D3 and an Ontario Graduate Scholarship. N.A. is supported by a scholarship from King Faisal Specialist Hospital and Research Center, Riyadh, Saudi Arabia (KFSHRC) representative by Saudi Arabian Cultural Bureau in Canada (SACB). BioRender was used to create the graphical abstract.

AUTHOR CONTRIBUTIONS

Conceptualization – S.B., J.P., R.S., M.J.F.C., N.M, T.J., T.A., C.S.I., and J.C.B. Methodology – S.B., J.P., N.A., M.J.F.C, L.A., and T.J. Investigation/data acquisition – S.B., R.G., N.A. X.H., J.P. B.A., Z.T., I.T., S.S., R.J., and R.M. Formal Analysis – S.B., J.P., R.G., N.A., and X.H. Project administration – S.B. and J.C.B. Supervision – J.-S.D., C.S.I. and J.C.B. Funding acquisition – C.S.I. and J.C.B. Visualization and writing of original draft – S.B. Reviewing and editing – all authors.

DECLARATION OF INTERESTS

All authors have declared that they have no conflicts of interest with this study.

REFERENCES

1. Zhang, Y., Banga Ndzouboukou, J.-L., Gan, M., Lin, X., and Fan, X. (2021). Immune Evasive Effects of SARS-CoV-2 Variants to COVID-19 Emergency Used Vaccines. Front. Immunol. *12*, 771242. https://doi.org/10.3389/fimmu.2021.771242.

2. Syed, A.M., Ciling, A., Taha, T.Y., Chen, I.P., Khalid, M.M., Sreekumar, B., Chen, P.-Y., Kumar, G.R., Suryawanshi, R., Silva, I., et al. (2022). Omicron mutations enhance infectivity and reduce antibody neutralization of SARS-CoV-2 virus-like particles. Proc. Natl. Acad. Sci. USA *119*, e2200592119. https://doi.org/10.1073/pnas.2200592119.

3. Chenchula, S., Karunakaran, P., Sharma, S., and Chavan, M. (2022). Current evidence on efficacy of COVID-19 booster dose vaccination against the Omicron variant: A systematic review. J. Med. Virol. *94*, 2969–2976. https://doi.org/10.1002/jmv.27697.

4. Hachmann, N.P., Miller, J., Collier, A.-R.Y., Ventura, J.D., Yu, J., Rowe, M., Bondzie, E.A., Powers, O., Surve, N., Hall, K., and Barouch, D.H. (2022). Neutralization Escape by SARS-CoV-2 Omicron Subvariants BA.2.12.1, BA.4, and BA.5. N. Engl. J. Med. *387*, 86–88. https://doi.org/10.1056/NEJMc2206576.

5. Offit, P.A. (2023). Bivalent Covid-19 Vaccines — A Cautionary Tale. N. Engl. J. Med. *388*, 481–483. https://doi.org/10.1056/NEJMp2215780.

6. Yao, L., Zhu, K.-L., Jiang, X.-L., Wang, X.-J., Zhan, B.-D., Gao, H.-X., Geng, X.-Y., Duan, L.-J., Dai, E.-H., and Ma, M.-J. (2022). Omicron subvariants escape antibodies elicited by vaccination and BA.2.2 infection. Lancet Infect. Dis. *22*, 1116–1117. https://doi.org/10.1016/S1473-3099(22)00410-8.

7. Jurdi, A.A., Gassen, R.B., Borges, T.J., Lape, I.T., Morena, L., Efe, O., Solhjou, Z., Fekih, R.E., Deban, C., Bohan, B., et al. (2022). Diminished antibody response against SARS-CoV-2 Omicron variant after third dose of mRNA vaccine in kidney transplant recipients. Preprint at medRxiv. https://doi.org/10.1101/2022.01.03.22268649.

8. Shoham, S., Batista, C., Ben Amor, Y., Ergonul, O., Hassanain, M., Hotez, P., Kang, G., Kim, J.H., Lall, B., Larson, H.J., et al. (2023). Vaccines and therapeutics for immunocompromised patients with COVID-19. eClinicalMedicine *59*, 101965. https://doi.org/10.1016/j.eclinm.2023.101965.

9. Azzolini, E., Pozzi, C., Germagnoli, L., Oresta, B., Carriglio, N., Calleri, M., Selmi, C., De Santis, M., Finazzi, S., Carlo-Stella, C., et al. (2022). mRNA COVID-19 vaccine booster fosters B- and T-cell responses in immunocompromised patients. Life Sci. Alliance *5*, e202201381. https://doi.org/10.26508/lsa.202201381.

10. Mathieu, E., Ritchie, H., Rodés-Guirao, L., Appel, C., Giattino, C., Joe, H., Macdonald, B., Dattani, S., Beltekian, D., Ortiz-Ospina, E., et al. (2020). Coronavirus Pandemic (COVID-19) (Our World in Data).

11. Lazarus, J.V., Wyka, K., White, T.M., Picchio, C.A., Gostin, L.O., Larson, H.J., Rabin, K., Ratzan, S.C., Kamarulzaman, A., and El-Mohandes, A. (2023). A survey of COVID-19 vaccine acceptance across 23 countries in 2022. Nat. Med. *29*, 366–375. https://doi.org/10.1038/s41591-022-02185-4.

12. Reza, H.M., Agarwal, V., Sultana, F., Bari, R., and Mobarak, A.M. (2022). Why are vaccination rates lower in low and middle income countries, and what can we do about it? Br. Med. J. *378*, e069506. https://doi.org/10.1136/bmj-2021-069506.

13. Boulton, S., Poutou, J., Martin, N.T., Azad, T., Singaravelu, R., Crupi, M.J.F., Jamieson, T., He, X., Marius, R., Petryk, J., et al. (2022). Single-dose replicating poxvirus vector-based RBD vaccine drives robust humoral and T cell immune response against SARS-CoV-2 infection. Mol. Ther. *30*, 1885–1896. https://doi.org/10.1016/j.ymthe.2021.10.008.

14. Lu, B., Yu, W., Huang, X., Wang, H., Liu, L., and Chen, Z. (2011). Mucosal Immunization Induces a Higher Level of Lasting Neutralizing Antibody Response in Mice by a Replication-Competent Smallpox Vaccine: Vaccinia Tiantan Strain. J. Biomed. Biotechnol. *2011*, 970424. https://doi.org/10.1155/2011/970424.

15. Sutter, G., Wyatt, L.S., Foley, P.L., Bennink, J.R., and Moss, B. (1994). A recombinant vector derived from the host range-restricted and highly attenuated MVA strain of vaccinia virus stimulates protective immunity in mice to influenza virus. Vaccine *12*, 1032–1040. https://doi.org/10.1016/0264-410x(94)90341-7.

16. Sutter, G., and Moss, B. (1992). Nonreplicating vaccinia vector efficiently expresses recombinant genes. Proc. Natl. Acad. Sci. USA *89*, 10847–10851. https://doi.org/10.1073/pnas.89.22.10847.

17. Drillien, R., Spehner, D., and Hanau, D. (2004). Modified vaccinia virus Ankara induces moderate activation of human dendritic cells. J. Gen. Virol. *85*, 2167–2175. https://doi.org/10.1099/vir.0.79998-0.

18. Ramírez, J.C., Gherardi, M.M., Rodríguez, D., and Esteban, M. (2000). Attenuated Modified Vaccinia Virus Ankara Can Be Used as an Immunizing Agent under Conditions of Preexisting Immunity to the Vector. J. Virol. *74*, 7651–7655. https://doi.org/10.1128/jvi.74.16.7651-7655.2000.

19. Kannanganat, S., Nigam, P., Velu, V., Earl, P.L., Lai, L., Chennareddi, L., Lawson, B., Wilson, R.L., Montefiori, D.C., Kozlowski, P.A., et al. (2010). Preexisting Vaccinia Virus Immunity Decreases SIV-Specific Cellular Immunity but Does Not Diminish Humoral Immunity and Efficacy of a DNA/MVA Vaccine. J. Immunol. *185*, 7262–7273. https://doi.org/10.4049/jimmunol.1000751.

20. Belyakov, I.M., Moss, B., Strober, W., and Berzofsky, J.A. (1999). Mucosal vaccination overcomes the barrier to recombinant vaccinia immunization caused by preexisting poxvirus immunity. Proc. Natl. Acad. Sci. USA *96*, 4512–4517. https://doi.org/10.1073/pnas.96.8.4512.

21. Essbauer, S., Meyer, H., Porsch-Ozcürümez, M., and Pfeffer, M. (2007). Long-Lasting Stability of Vaccinia Virus (Orthopoxvirus) in Food and Environmental Samples. Zoonoses Public Health *54*, 118–124. https://doi.org/10.1111/j.1863-2378.2007.01035.x.

22. Newman, F.K., Frey, S.E., Blevins, T.P., Yan, L., Belshe, R.B., and Belshe, R.B. (2003). Stability of Undiluted and Diluted Vaccinia-Virus Vaccine, Dryvax. J. Infect. Dis. *187*, 1319–1322. https://doi.org/10.1086/374564.

23. Chen, Y., Liao, Q., Chen, T., Zhang, Y., Yuan, W., Xu, J., and Zhang, X. (2021). Freeze-Drying Formulations Increased the Adenovirus and Poxvirus Vaccine Storage Times

and Antigen Stabilities. Virol. Sin. *36*, 365–372. https://doi.org/10.1007/s12250-020-00250-1.

24. Jacobs, B.L., Langland, J.O., Kibler, K.V., Denzler, K.L., White, S.D., Holechek, S.A., Wong, S., Huynh, T., and Baskin, C.R. (2009). Vaccinia virus vaccines: Past, present and future. Antivir. Res. *84*, 1–13. https://doi.org/10.1016/j.antiviral.2009.06.006.

25. Huang, X., Lu, B., Yu, W., Fang, Q., Liu, L., Zhuang, K., Shen, T., Wang, H., Tian, P., Zhang, L., and Chen, Z. (2009). A Novel Replication-Competent Vaccinia Vector MVTT Is Superior to MVA for Inducing High Levels of Neutralizing Antibody via Mucosal Vaccination. PLoS One *4*, e4180. https://doi.org/10.1371/journal.pone.0004180.

26. Robert-Guroff, M. (2007). Replicating and non-replicating viral vectors for vaccine development. Curr. Opin. Biotechnol. *18*, 546–556. https://doi.org/10.1016/j.copbio.2007.10.010.

27. Peng, B., Wang, L.R., Gómez-Román, V.R., Davis-Warren, A., Montefiori, D.C., Kalyanaraman, V.S., Venzon, D., Zhao, J., Kan, E., Rowell, T.J., et al. (2005). Replicating Rather than Nonreplicating Adenovirus-Human Immunodeficiency Virus Recombinant Vaccines Are Better at Eliciting Potent Cellular Immunity and Priming High-Titer Antibodies. J. Virol. *79*, 10200–10209. https://doi.org/10.1128/JVI.79.16.10200-10209.2005.

28. Chavda, V.P., Bezbaruah, R., Athalye, M., Parikh, P.K., Chhipa, A.S., Patel, S., and Apostolopoulos, V. (2022). Replicating Viral Vector-Based Vaccines for COVID-19: Potential Avenue in Vaccination Arena. Viruses *14*, 759. https://doi.org/10.3390/v14040759.

29. Wan, Y.Y. (2010). Multi-tasking of helper T cells. Immunology *130*, 166–171. https://doi.org/10.1111/j.1365-2567.2010.03289.x.

30. Rydyznski Moderbacher, C., Ramirez, S.I., Dan, J.M., Grifoni, A., Hastie, K.M., Weiskopf, D., Belanger, S., Abbott, R.K., Kim, C., Choi, J., et al. (2020). Antigen-Specific Adaptive Immunity to SARS-CoV-2 in Acute COVID-19 and Associations with Age and Disease Severity. Cell *183*, 996–1012.e19. https://doi.org/10.1016/j.cell.2020.09.038.

31. Baumjohann, D., and Fazilleau, N. (2021). Antigen-dependent multistep differentiation of T follicular helper cells and its role in SARS-CoV-2 infection and vaccination. Eur. J. Immunol. *51*, 1325–1333. https://doi.org/10.1002/eji.202049148.

32. Wragg, K.M., Lee, W.S., Koutsakos, M., Tan, H.-X., Amarasena, T., Reynaldi, A., Gare, G., Konstandopoulos, P., Field, K.R., Esterbauer, R., et al. (2022). Establishment and recall of SARS-CoV-2 spike epitope-specific CD4+ T cell memory. Nat. Immunol. *23*, 768–780. https://doi.org/10.1038/s41590-022-01175-5.

33. Grifoni, A., Weiskopf, D., Ramirez, S.I., Mateus, J., Dan, J.M., Moderbacher, C.R., Rawlings, S.A., Sutherland, A., Premkumar, L., Jadi, R.S., et al. (2020). Targets of T Cell Responses to SARS-CoV-2 Coronavirus in Humans with COVID-19 Disease and Unexposed Individuals. Cell *181*, 1489–1501.e15. https://doi.org/10.1016/j.cell.2020.05.015.

34. Nelde, A., Bilich, T., Heitmann, J.S., Maringer, Y., Salih, H.R., Roerden, M., Lübke, M., Bauer, J., Rieth, J., Wacker, M., et al. (2021). SARS-CoV-2-derived peptides define heterologous and COVID-19-induced T cell recognition. Nat. Immunol. *22*, 74–85. https://doi.org/10.1038/s41590-020-00808-x.

35. Shomuradova, A.S., Vagida, M.S., Sheetikov, S.A., Zornikova, K.V., Kiryukhin, D., Titov, A., Peshkova, I.O., Khmelevskaya, A., Dianov, D.V., Malasheva, M., et al. (2020). SARS-CoV-2 Epitopes Are Recognized by a Public and Diverse Repertoire of Human T Cell Receptors. Immunity *53*, 1245–1257.e5. https://doi.org/10.1016/j.immuni.2020.11.004.

36. Abd El-Baky, N., Amara, A.A., and Redwan, E.M. (2023). HLA-I and HLA-II Peptidomes of SARS-CoV-2: A Review. Vaccines *11*, 548. https://doi.org/10.3390/vaccines11030548.

37. Tarke, A., Sidney, J., Kidd, C.K., Dan, J.M., Ramirez, S.I., Yu, E.D., Mateus, J., da Silva Antunes, R., Moore, E., Rubiro, P., et al. (2021). Comprehensive analysis of T cell immunodominance and immunoprevalence of SARS-CoV-2 epitopes in COVID-19 cases. Cell Rep. Med. *2*, 100204. https://doi.org/10.1016/j.xcrm.2021.100204.

38. Nagler, A., Kalaora, S., Barbolin, C., Gangaev, A., Ketelaars, S.L.C., Alon, M., Pai, J., Benedek, G., Yahalom-Ronen, Y., Erez, N., et al. (2021). Identification of presented SARS-CoV-2 HLA class I and HLA class II peptides using HLA peptidomics. Cell Rep. *35*, 109305. https://doi.org/10.1016/j.celrep.2021.109305.

39. Le Bert, N., Tan, A.T., Kunasegaran, K., Tham, C.Y.L., Hafezi, M., Chia, A., Chng, M.H.Y., Lin, M., Tan, N., Linster, M., et al. (2020). SARS-CoV-2-specific T cell immunity in cases of COVID-19 and SARS, and uninfected controls. Nature *584*, 457–462. https://doi.org/10.1038/s41586-020-2550-z.

40. Dutta, N.K., Mazumdar, K., and Gordy, J.T. (2020). The Nucleocapsid Protein of SARS–CoV-2: a Target for Vaccine Development. J. Virol. *94*, e00647-20. https://doi.org/10.1128/JVI.00647-20.

41. Oronsky, B., Larson, C., Caroen, S., Hedjran, F., Sanchez, A., Prokopenko, E., and Reid, T. (2022). Nucleocapsid as a next-generation COVID-19 vaccine candidate. Int. J. Infect. Dis. *122*, 529–530. https://doi.org/10.1016/j.ijid.2022.06.046.

42. Thomson, S.A., Khanna, R., Gardner, J., Burrows, S.R., Coupar, B., Moss, D.J., and Suhrbier, A. (1995). Minimal epitopes expressed in a recombinant polyepitope protein are processed and presented to CD8+ cytotoxic T cells: implications for vaccine design. Proc. Natl. Acad. Sci. USA *92*, 5845–5849. https://doi.org/10.1073/pnas.92.13.5845.

43. Thomson, S.A., Burrows, S.R., Misko, I.S., Moss, D.J., Coupar, B.E., and Khanna, R. (1998). Targeting a Polyepitope Protein Incorporating Multiple Class II-Restricted Viral Epitopes to the Secretory/Endocytic Pathway Facilitates Immune Recognition by CD4 + Cytotoxic T Lymphocytes: a Novel Approach to Vaccine Design. J. Virol. *72*, 2246–2252. https://doi.org/10.1128/JVI.72.3.2246-2252.1998.

44. Zhang, L. (2018). Multi-epitope vaccines: a promising strategy against tumors and viral infections. Cell. Mol. Immunol. *15*, 182–184. https://doi.org/10.1038/cmi.2017.92.

45. Velders, M.P., Weijzen, S., Eiben, G.L., Elmishad, A.G., Kloetzel, P.-M., Higgins, T., Ciccarelli, R.B., Evans, M., Man, S., Smith, L., and Kast, W.M. (2001). Defined Flanking Spacers and Enhanced Proteolysis Is Essential for Eradication of Established Tumors by an Epitope String DNA Vaccine. J. Immunol. *166*, 5366–5373. https://doi.org/10.4049/jimmunol.166.9.5366.

46. Cubuk, J., Alston, J.J., Incicco, J.J., Singh, S., Stuchell-Brereton, M.D., Ward, M.D., Zimmerman, M.I., Vithani, N., Griffith, D., Wagoner, J.A., et al. (2021). The SARS-CoV-2 nucleocapsid protein is dynamic, disordered, and phase separates with RNA. Nat. Commun. *12*, 1936. https://doi.org/10.1038/s41467-021-21953-3.

47. Wang, S., Dai, T., Qin, Z., Pan, T., Chu, F., Lou, L., Zhang, L., Yang, B., Huang, H., Lu, H., and Zhou, F. (2021). Targeting liquid–liquid phase separation of SARS-CoV-2 nucleocapsid protein promotes innate antiviral immunity by elevating MAVS activity. Nat. Cell Biol. *23*, 718–732. https://doi.org/10.1038/s41556-021-00710-0.

48. Wu, C., Qavi, A.J., Hachim, A., Kavian, N., Cole, A.R., Moyle, A.B., Wagner, N.D., Sweeney-Gibbons, J., Rohrs, H.W., Gross, M.L., et al. (2021). Characterization of SARS-CoV-2 nucleocapsid protein reveals multiple functional consequences of the C-terminal domain. iScience *24*, 102681. https://doi.org/10.1016/j.isci.2021.102681.

49. Symons, J.A., Tscharke, D.C., Price, N., and Smith, G.L. (2002). A study of the vaccinia virus interferon-γ receptor and its contribution to virus virulence. J. Gen. Virol. *83*, 1953–1964. https://doi.org/10.1099/0022-1317-83-8-1953.

50. Verardi, P.H., Jones, L.A., Aziz, F.H., Ahmad, S., and Yilma, T.D. (2001). Vaccinia Virus Vectors with an Inactivated Gamma Interferon Receptor Homolog Gene (B8R) Are Attenuated In Vivo without a Concomitant Reduction in Immunogenicity. J. Virol. *75*, 11–18. https://doi.org/10.1128/JVI.75.1.11-18.2001.

51. Diethelm-Okita, B.M., Okita, D.K., Banaszak, L., and Conti-Fine, B.M. (2000). Universal Epitopes for Human CD4 + Cells on Tetanus and Diphtheria Toxins. J. Infect. Dis. *181*, 1001–1009. https://doi.org/10.1086/315324.

52. Diethelm-Okita, B.M., Raju, R., Okita, D.K., and Conti-Fine, B.M. (1997). Epitope Repertoire of Human CD4+ T Cells on Tetanus Toxin: Identification of Immunodominant Sequence Segments. J. Infect. Dis. *175*, 382–391. https://doi.org/10.1093/infdis/175.2.382.

53. Laubreton, D., Bay, S., Sedlik, C., Artaud, C., Ganneau, C., Dériaud, E., Viel, S., Puaux, A.-L., Amigorena, S., Gérard, C., et al. (2016). The fully synthetic MAG-Tn3 therapeutic vaccine containing the tetanus toxoid-derived TT830-844 universal epitope provides anti-tumor immunity. Cancer Immunol. Immunother. *65*, 315–325. https://doi.org/10.1007/s00262-016-1802-0.

54. Rodriguez, F., An, L.L., Harkins, S., Zhang, J., Yokoyama, M., Widera, G., Fuller, J.T., Kincaid, C., Campbell, I.L., and Whitton, J.L. (1998). DNA Immunization with Minigenes: Low Frequency of Memory Cytotoxic T Lymphocytes and Inefficient Antiviral Protection Are Rectified by Ubiquitination. J. Virol. *72*, 5174–5181.

55. Buller, R.M., Smith, G.L., Cremer, K., Notkins, A.L., and Moss, B. (1985). Decreased virulence of recombinant vaccinia virus expression vectors is associated with a thymidine kinase-negative phenotype. Nature *317*, 813–815. https://doi.org/10.1038/317813a0.

56. Scheiflinger, F., Falkner, F.G., and Dorner, F. (1996). Evaluation of the thymidine kinase (tk) locus as an insertion site in the highly attenuated vaccinia MVA strain. Arch. Virol. *141*, 663–669. https://doi.org/10.1007/BF01718324.

57. Kang, S., Yang, M., He, S., Wang, Y., Chen, X., Chen, Y.-Q., Hong, Z., Liu, J., Jiang, G., Chen, Q., et al. (2021). A SARS-CoV-2 antibody curbs viral nucleocapsid protein-induced complement hyperactivation. Nat. Commun. *12*, 2697. https://doi.org/10.1038/s41467-021-23036-9.

58. Nakayama, E.E., Kubota-Koketsu, R., Sasaki, T., Suzuki, K., Uno, K., Shimizu, J., Okamoto, T., Matsumoto, H., Matsuura, H., Hashimoto, S., et al. (2022). Anti-nucleocapsid antibodies enhance the production of IL-6 induced by SARS-CoV-2 N protein. Sci. Rep. *12*, 8108. https://doi.org/10.1038/s41598-022-12252-y.

59. Zhang, Z., Dong, L., Zhao, C., Zheng, P., Zhang, X., and Xu, J. (2021). J. Vaccinia virus-based vector against infectious diseases and tumors. Hum. Vaccines Immunother. *17*, 1578–1585. https://doi.org/10.1080/21645515.2020.1840887.

60. Mackett, M., Smith, G.L., and Moss, B. (1982). Vaccinia virus: a selectable eukaryotic cloning and expression vector. Proc. Natl. Acad. Sci. USA *79*, 7415–7419. https://doi.org/10.1073/pnas.79.23.7415.

61. Altenburger, W., Süter, C.P., and Altenburger, J. (1989). Partial deletion of the human host range gene in the attenuated vaccinia virus MVA. Arch. Virol. *105*, 15–27. https://doi.org/10.1007/BF01311113.

62. Meyer, H., Sutter, G., and Mayr, A. (1991). Mapping of deletions in the genome of the highly attenuated vaccinia virus MVA and their influence on virulence. J. Gen. Virol. *72*, 1031–1038. https://doi.org/10.1099/0022-1317-72-5-1031.

63. Herman, J.D., Wang, C., Burke, J.S., Zur, Y., Compere, H., Kang, J., Macvicar, R., Taylor, S., Shin, S., Frank, I., et al. (2022). Nucleocapsid-specific antibody function is associated with therapeutic benefits from COVID-19 convalescent plasma therapy. Cell Rep. Med. *3*, 100811. https://doi.org/10.1016/j.xcrm.2022.100811.

64. Gao, T., Zhu, L., Liu, H., Zhang, X., Wang, T., Fu, Y., Li, H., Dong, Q., Hu, Y., Zhang, Z., et al. (2022). Highly pathogenic coronavirus N protein aggravates inflammation by MASP-2-mediated lectin complement pathway overactivation. Signal Transduct. Targeted Ther. *7*, 318. https://doi.org/10.1038/s41392-022-01133-5.

65. Chandrasekar, S.S., Phanse, Y., Hildebrand, R.E., Hanafy, M., Wu, C.-W., Hansen, C.H., Osorio, J.E., Suresh, M., and Talaat, A.M. (2021). Localized and Systemic Immune Responses against SARS-CoV-2 Following Mucosal Immunization. Vaccines *9*, 132. https://doi.org/10.3390/vaccines9020132.

66. Ryzhikov, A.B., Ryzhikov, E.A., Bogryantseva, M.P., Usova, S.V., Danilenko, E.D., Nechaeva, E.A., Pyankov, O.V., Pyankova, O.G., Gudymo, A.S., Bodnev, S.A., et al. (2021). A single blind, placebo-controlled randomized study of the safety, reactogenicity and immunogenicity of the "EpiVacCorona" Vaccine for the prevention of COVID-19, in volunteers aged 18–60 years (phase I–II). Russian Journal of Infection and Immunity *11*, 283–296. https://doi.org/10.15789/2220-7619-ASB-1699.

67. Arieta, C.M., Xie, Y.J., Rothenberg, D.A., Diao, H., Harjanto, D., Meda, S., Marquart, K., Koenitzer, B., Sciuto, T.E., Lobo, A., et al. (2023). The T-cell-directed vaccine BNT162b4 encoding conserved non-spike antigens protects animals from severe SARS-CoV-2 infection. Cell *186*, 2392–2409.e21. https://doi.org/10.1016/j.cell.2023.04.007.

68. Chiuppesi, F., Salazar, M.d., Contreras, H., Nguyen, V.H., Martinez, J., Park, Y., Nguyen, J., Kha, M., Iniguez, A., Zhou, Q., et al. (2020). Development of a multi-antigenic SARS-CoV-2 vaccine candidate using a synthetic poxvirus platform. Nat. Commun. *11*, 6121. https://doi.org/10.1038/s41467-020-19819-1.

69. O'Donnell, K.L., Gourdine, T., Fletcher, P., Clancy, C.S., and Marzi, A. (2022). Protection from COVID-19 with a VSV-based vaccine expressing the spike and nucleocapsid proteins. Front. Immunol. *13*, 1025500. https://doi.org/10.3389/fimmu.2022.1025500.

70. Matchett, W.E., Joag, V., Stolley, J.M., Shepherd, F.K., Quarnstrom, C.F., Mickelson, C.K., Wijeyesinghe, S., Soerens, A.G., Becker, S., Thiede, J.M., et al. (2021). Cutting Edge: Nucleocapsid Vaccine Elicits Spike-Independent SARS-CoV-2 Protective Immunity. J. Immunol. *207*, 376–379. https://doi.org/10.4049/jimmunol.2100421.

71. Panina-Bordignon, P., Tan, A., Termijtelen, A., Demotz, S., Corradin, G., and Lanzavecchia, A. (1989). Universally immunogenic T cell epitopes: promiscuous binding to human MHC class II and promiscuous recognition by T cells. Eur. J. Immunol. *19*, 2237–2242. https://doi.org/10.1002/eji.1830191209.

72. Hamley, I.W. (2022). Peptides for Vaccine Development. ACS Appl. Bio Mater. *5*, 905–944. https://doi.org/10.1021/acsabm.1c01238.

73. Trougakos, I.P., Terpos, E., Alexopoulos, H., Politou, M., Paraskevis, D., Scorilas, A., Kastritis, E., Andreakos, E., and Dimopoulos, M.A. (2022). Adverse effects of COVID-19 mRNA vaccines: the spike hypothesis. Trends Mol. Med. *28*, 542–554. https://doi.org/10.1016/j.molmed.2022.04.007.

74. Yahi, N., Chahinian, H., and Fantini, J. (2021). Infection-enhancing anti-SARS-CoV-2 antibodies recognize both the original Wuhan/D614G strain and Delta variants. A potential risk for mass vaccination? J. Infect. *83*, 607–635. https://doi.org/10.1016/j.jinf.2021.08.010.

75. Rajah, M.M., Bernier, A., Buchrieser, J., and Schwartz, O. (2022). The Mechanism and Consequences of SARS-CoV-2 Spike-Mediated Fusion and Syncytia Formation. J. Mol. Biol. *434*, 167280. https://doi.org/10.1016/j.jmb.2021.167280.

76. Navaratnarajah, C.K., Pease, D.R., Halfmann, P.J., Taye, B., Barkhymer, A., Howell, K.G., Charlesworth, J.E., Christensen, T.A., Kawaoka, Y., Cattaneo, R., et al. (2021). Highly Efficient SARS-CoV-2 Infection of Human Cardiomyocytes: Spike Protein-Mediated Cell Fusion and Its Inhibition. J. Virol. *95*, e0136821. https://doi.org/10.1128/JVI.01368-21.

77. Rzymski, P., Camargo, C.A., Fal, A., Flisiak, R., Gwenzi, W., Kelishadi, R., Leemans, A., Nieto, J.J., Ozen, A., Perc, M., et al. (2021). COVID-19 Vaccine Boosters: The Good, the Bad, and the Ugly. Vaccines *9*, 1299. https://doi.org/10.3390/vaccines9111299.

78. Kraay, A.N.M., Gallagher, M.E., Ge, Y., Han, P., Baker, J.M., Koelle, K., Handel, A., and Lopman, B.A. (2022). The role of booster vaccination and ongoing viral evolution in seasonal circulation of SARS-CoV-2. J. R. Soc. Interface *19*, 20220477. https://doi.org/10.1098/rsif.2022.0477.

79. Rubin, R. (2021). COVID-19 Vaccine Makers Plan for Annual Boosters, but It's Not Clear They'll Be Needed. JAMA *326*, 2247–2249. https://doi.org/10.1001/jama.2021.21291.

80. Case, J.B., Rothlauf, P.W., Chen, R.E., Liu, Z., Zhao, H., Kim, A.S., Bloyet, L.-M., Zeng, Q., Tahan, S., Droit, L., et al. (2020). Neutralizing Antibody and Soluble ACE2 Inhibition of a Replication-Competent VSV-SARS-CoV-2 and a Clinical Isolate of SARS-CoV-2. Cell Host Microbe *28*, 475–485.e5. https://doi.org/10.1016/j.chom.2020.06.021.

81. Qin, L., and Evans, D.H. (2014). Genome Scale Patterns of Recombination between Coinfecting Vaccinia Viruses. J. Virol. *88*, 5277–5286. https://doi.org/10.1128/JVI.00022-14.

82. Stojdl, D.F., Lichty, B.D., tenOever, B.R., Paterson, J.M., Power, A.T., Knowles, S., Marius, R., Reynard, J., Poliquin, L., Atkins, H., et al. (2003). VSV strains with defects in their ability to shutdown innate immunity are potent systemic anti-cancer agents. Cancer Cell *4*, 263–275. https://doi.org/10.1016/s1535-6108(03)00241-1.

83. Flesch, I.E.A., Woo, W.-P., Wang, Y., Panchanathan, V., Wong, Y.-C., La Gruta, N.L., Cukalac, T., and Tscharke, D.C. (2010). Altered CD8+ T Cell Immunodominance after Vaccinia Virus Infection and the Naive Repertoire in Inbred and F1 Mice. J. Immunol. *184*, 45–55. https://doi.org/10.4049/jimmunol.0900999.

84. Breitbach, C.J., De Silva, N.S., Daneshmand, M., Falls, T.J., Aladl, U., Evgin, L., Paterson, J., Sun, Y.Y., Roy, D.G., Rintoul, J.L., and Daneshmand, M. (2011). Targeting Tumor Vasculature With an Oncolytic Virus. Mol. Ther. *19*, 886–894. https://doi.org/10.1038/mt.2011.26.